REFERENCES

[1] Zhang, S., Xu, H., Zhang, L. and Qiao, Y., 2020. Cervical cancer: Epidemiology, risk factors and screening. *Chinese Journal of Cancer Research*, *32*(6), pp.720-728. DOI: 10.21147/j.issn.1000-9604.2020.06.05.

[2] World Health Organization 2024, *Cervical Cancer*, viewed 22 April 2024, (https://www.who.int/news-room/fact-sheets/detail/cervical-cancer/).

[3] Rashid, S., Labani, S. and Das, B.C., 2016. Knowledge, awareness and attitude on HPV, HPV vaccine and cervical cancer among the college students in India. *PloS one*, *11*(11), p.e0166713. DOI: 10.1371/journal.pone.0166713

[4] Ghosh, S., Mallya, S.D., Shetty, R.S., Pattanshetty, S.M., Pandey, D., Kabekkodu, S.P., Satyamoorthy, K. and Kamath, V.G., 2021. Knowledge, attitude and practices towards cervical cancer and its screening among women from tribal population: A community-based study from southern India. *Journal of racial and ethnic health disparities*, *8*, pp.88-93. DOI: 10.1007/s40615-020-00760-4.

[5] Petignat, P. and Roy, M., 2007. Diagnosis and management of cervical cancer. *Bmj*, *335*(7623), pp.765-768. DOI: 10.1136/bmj.39337.615197.80.

[6] Schiffman, M., Castle, P.E., Jeronimo, J., Rodriguez, A.C. and Wacholder, S., 2007. Human papillomavirus and cervical cancer. *The lancet*, *370*(9590), pp.890-907.DOI: 10.1128/CMR.16.1.1-17.2003.

[7] Ahmed, H.G., Bensumaidea, S.H., Alshammari, F.D., Alenazi, F.S.H., ALmutlaq, B.A., Alturkstani, M.Z. and Aladani, I.A., 2017. Prevalence of human papillomavirus subtypes 16 and 18 among Yemeni patients with cervical cancer. *Asian Pacific journal of cancer prevention: APJCP*, *18*(6), p.1543. DOI: 10.22034/APJCP.2017. 18.6.1543.

[8] Hull, R., Mbele, M., Makhafola, T., Hicks, C., Wang, S.M., Reis, R.M., Mehrotra, R., Mkhize-Kwitshana, Z., Kibiki, G., Bates, D.O. and Dlamini, Z., 2020. Cervical cancer in low and middle-income countries. *Oncology letters*, *20*(3), pp.2058-2074. DOI: 10.3892/ol.2020.11754.

[9] World Health Organization 2020, *WHO releases new estimates of Global burden of Cervical cancer associated with HIV*, viewed 22 April 2024, (https://www.who.int/news/item/16-11-2020-who-releases-new-estimates-of-the-global-burden-of-cervical-cancer-associated-with-hiv/).

[10] Poondla, N., Madduru, D., Duppala, S.K., Velpula, S., Nunia, V., Kharb, S., Ghatak, S., Mishra, A.K., Vuree, S., Neyaz, M.K. and Suravajhala, P., 2021. Cervical cancer in the era of precision medicine: A perspective from developing countries. *Advances in Cancer Biology-Metastasis*, *3*, p.100015. DOI: 10.1016/j.adcanc.2021.100015.

[11] Lee, N.C., Wong, F.L., Jamison, P.M., Jones, S.F., Galaska, L., Brady, K.T., Wethers, B. and Stokes-Townsend, G.A., 2014. Implementation of the national breast and cervical cancer early detection program: the beginning. *Cancer*, *120*(S16), pp.2540-2548. DOI: 10.1002/cncr.28820.

[12] Rahman, M., Mia, A.R., Haque, S.E., Golam, M., Purabi, N.S. and Choudhury, S.A.R., 2013. Beating Cervical Cancer in the Developed Countries: A Dream or a Reality?. *Alfonso J. Rodriguez-Morales. Current Topics in Public Health. IntechOpen*, pp.341-58. DOI: 10.5772/52881.

[13] Ghosh, S., Pattanshetty, S.M., Mallya, S.D., Pandey, D., Guddattu, V., Kamath, V.G., Kabekkodu, S.P., Satyamoorthy, K. and Shetty, R.S., 2021. Cervical cytology and associated factors among tribal women of Karnataka, India. *Plos one*, *16*(3), p.e0248963.DOI: 10.1371/journal.pone.0248963.

[14] Habtu, Y., Yohannes, S. and Laelago, T., 2018. Health seeking behavior and its determinants for cervical cancer among women of childbearing age in Hossana Town, Hadiya zone, Southern Ethiopia: community based cross sectional study. *BMC cancer*, *18*, pp.1-9. DOI: 10.1186/s12885-018-4203-2.

[15] Novais, I.R., Coelho, C.O., Machado, H.C., Surita, F., Zeferino, L.C. and Vale, D.B., 2023. Cervical cancer screening in Brazilian Amazon Indigenous women: Towards the intensification of public policies for prevention. *Plos one*, *18*(12), p.e0294956.DOI: 10.1371/journal.pone.0294956.

[16] Brito, E.B., Martins, S.J. and Menezes, R.C., 2002. Human papillomaviruses in Amerindian women from Brazilian Amazonia. *Epidemiology & Infection*, *128*(3), pp.485-489.DOI: 10.1017/S0950268802006908.

[17] Ezechi, O.C., Gab-Okafor, C.V., Ostergren, P.O. and Odberg Pettersson, K., 2013. Willingness and acceptability of cervical cancer screening among HIV positive Nigerian women. *BMC Public Health*, *13*, pp.1-8.DOI: 10.1186/1471-2458-13-46.

[18] Lidofsky, A., Miller, A., Jorgensen, J., Tajik, A., Tendeu, K., Pius, D., Mallange, E. and Dougherty, A., 2019. Development and implementation of a culturally appropriate education program to increase cervical cancer screening among Maasai women in rural Tanzania. *Annals of Global Health*, *85*(1). DOI: 10.5334/aogh.2503.

[19] Poli, U.R., Bidinger, P.D. and Gowrishankar, S., 2015. Visual inspection with acetic acid (via) screening program: 7 years experience in early detection of cervical cancer and pre-cancers in rural South India. *Indian Journal of Community Medicine*, *40*(3), pp.203-207. DOI: 10.4103/0970-0218.158873

[20] Ghosh, P., Gandhi, G., Kochhar, P.K., Zutshi, V. and Batra, S., 2012. Visual inspection of cervix with Lugol's iodine for early detection of premalignant & malignant lesions of cervix. *Indian Journal of Medical Research*, *136*(2), pp.265-271.

[21] Khan, M., Sultana, S.S., Jabeen, N., Arain, U. and Khan, S., 2015. Visual inspection of cervix with acetic acid: a good alternative to pap smear for cervical cancer screening in resource-limited setting. *J Pak Med Assoc*, 65(2), pp.192-195.

[22] Sankaranarayanan, R., Nessa, A., Esmy, P.O. and Dangou, J.M., 2012. Visual inspection methods for cervical cancer prevention. *Best practice & research Clinical obstetrics & gynaecology*, *26*(2), pp.221-232. DOI: 10.1016/j.bpobgyn.2011.08.003.

[23] Sarian, L.O., Derchain, S.F., Naud, P., Roteli-Martins, C., Longatto-Filho, A., Tatti, S., Branca, M., Eržen, M., Serpa-Hammes, L., Matos, J. and Gontijo, R.C., 2005. Evaluation of visual inspection with acetic acid (VIA), Lugol's iodine (VILI), cervical cytology and HPV testing as cervical screening tools in Latin America: This report refers to partial results from the LAMS (Latin AMerican Screening) study. *Journal of medical screening*, *12*(3), pp.142-149. DOI: 10.1258/0969141054855328

[24] Qiao, L., Li, B., Long, M., Wang, X., Wang, A. and Zhang, G., 2015. Accuracy of visual inspection with acetic acid and with Lugol's iodine for cervical cancer screening: Meta-analysis. *Journal of Obstetrics and Gynaecology Research*, *41*(9), pp.1313-1325. DOI: 10.1111/jog.12732.

[25] Sachan, P.L., Singh, M., Patel, M.L. and Sachan, R., 2018. A study on cervical cancer screening using pap smear test and clinical correlation. *Asia-Pacific journal of oncology nursing*, *5*(3), pp.337-341. DOI: 10.4103/apjon.apjon_15_18.

[26] Nkwabong, E., Laure Bessi Badjan, I. and Sando, Z., 2019. Pap smear accuracy for the diagnosis of cervical precancerous lesions. *Tropical Doctor*, *49*(1), pp.34-39. DOI: 10.1177/0049475518798532

[27] Sirovich, B.E. and Welch, H.G., 2004. The frequency of Pap smear screening in the United States. *Journal of general internal medicine*, *19*, pp.243-250. DOI:10.1111/j.1525-1497.2004.21107.x

[28] Cox, J.T., 2004. Liquid-based cytology: evaluation of effectiveness, cost-effectiveness, and application to present practice. *Journal of the National Comprehensive Cancer Network*, *2*(6), pp.597-611. DOI: 10.6004/jnccn.2004.0050

[29] Doyle, B., O'farrell, C., Mahoney, E., Turner, L., Magee, D. and Gibbons, D., 2006. Liquid-based cytology improves productivity in cervical cytology screening. *Cytopathology*, *17*(2), pp.60-64. DOI: 10.1111/j.1365-2303.2006.00338.x

[30] Cioc, A.M., Julius, C.J., Proca, D.M., Tranovich, V.L. and Keyhani-Rofagha, S., 2002. Cervical biopsy/cytology correlation data can be collected prospectively and shared clinically. *Diagnostic cytopathology*, *26*(1), pp.49-52. DOI: 10.1002/dc.10036

[31] Reyes, M.C. and Cooper, K., 2014. Cervical cancer biopsy reporting: A review. *Indian Journal of Pathology and Microbiology*, *57*(3), pp.364-368. DOI:10.4103/0377-4929.138713

[32] Kim, M.K., Kim, M.A., Kim, J.W., Chung, H.H., Park, N.H., Song, Y.S. and Kang, S.B., 2012. Loop electrosurgical excision procedure findings for identification of patients with early-stage cervical cancer suitable for less radical surgery. *International Journal of Gynecologic Cancer*, *22*(7), pp. 1214-1219. DOI: 10.1097/IGC.0b013e31825fb63b.

[33] D'Alessandro, P., Arduino, B., Borgo, M., Saccone, G., Venturella, R., Di Cello, A. and Zullo, F., 2018. Loop electrosurgical excision procedure versus cryotherapy in the treatment of cervical intraepithelial neoplasia: a systematic review and meta-analysis of randomized controlled trials. *Gynecology and minimally invasive therapy*, *7*(4), pp.145-151. DOI: 10.4103/GMIT.GMIT_56_18.

[34] Zuchna, C., Hager, M., Tringler, B., Georgoulopoulos, A., Ciresa-Koenig, A., Volgger, B., Widschwendter, A. and Staudach, A., 2010. Diagnostic accuracy of guided cervical biopsies: a prospective multicenter study comparing the histopathology of simultaneous biopsy and cone specimen. *American journal of obstetrics and gynecology*, *203*(4), pp.321.e1-321.e6. DOI: 10.1016/j.ajog.2010.05.033

[35] Giannella, L., Mfuta, K., Gardini, G., Rubino, T., Fodero, C. and Prandi, S., 2015. High-grade CIN on cervical biopsy and predictors of the subsequent cone histology results in women undergoing immediate conization. *European Journal of Obstetrics & Gynecology and Reproductive Biology*, *186*, pp.68-74. DOI: 10.1016/j.ejogrb.2015.01.015

[36] Arbyn, M., Simon, M., Peeters, E., Xu, L., Meijer, C.J., Berkhof, J., Cuschieri, K., Bonde, J., Vanlencak, A.O., Zhao, F.H. and Rezhake, R., 2021. 2020 list of human papillomavirus assays suitable for primary cervical cancer screening. *Clinical Microbiology and Infection*, *27*(8), pp.1083-1095. DOI: 10.1016/j.cmi.2021.04.031

[37] Fernandes, K., Cardoso, J.S. and Fernandes, J., 2018. Automated methods for the decision support of cervical cancer screening using digital colposcopies. *Ieee Access*, *6*, pp.33910-33927. DOI: 10.1109/ACCESS.2018.2839338

[38] Hermens, M., Ebisch, R.M., Galaal, K. and Bekkers, R.L., 2016. Alternative colposcopy techniques: a systematic review and meta-analysis. *Obstetrics & Gynecology*, *128*(4), pp.795-803. DOI: 10.1097/AOG.0000000000001613

[39] Mink, J. and Peterson, C., 2016. MobileODT: a case study of a novel approach to an mHealth-based model of sustainable impact. *Mhealth*, *2*(4), pp. 2-12 DOI: 10.21037/mhealth.2016.03.10.

[40] Castor, D., Saidu, R., Boa, R., Mbatani, N., Mutsvangwa, T.E., Moodley, J., Denny, L. and Kuhn, L., 2022. Assessment of the implementation context in preparation for a clinical study of machine-learning algorithms to automate the classification of digital cervical images for cervical cancer screening in resource-constrained settings. *Frontiers in Health Services*, *2*, p.1000150.S. DOI: 10.3389/ frhs.2022.1000150.

[41] Parvez, R., Hedau, S., Bhattacharya, D., Bhattacharjee, H., Muruganandam, N., Das, B.C., Saha, M.K., Sugunan, A.P. and Vijayachari, P., 2012. High-risk HPV infection among the tribal and non-tribal women of the Andaman and Nicobar Islands, India. *public health*, *126*(1), pp.67-69. DOI: 10.1016/j.puhe.2011.09.018.

[42] George, TJ., 2021. Factors influencing utilization of cervical cancer screening services among women – A cross sectional survey. *Clinical Epidemiology and Global Health,* 11:100752. DOI: 10.1016/j.cegh.2021.100752.

[43] Patil, A.D., Salvi, N.R., Shahina, B., Pimple, A.S., Mishra, A.G., Chauhan, L.S. and Joshi, B.N., 2019. Perspectives of primary healthcare providers on implementing cancer screening services in tribal block of Maharashtra, India. *South Asian journal of cancer*, *8*(03), pp.145-149. DOI: 10.4103/sajc.sajc_290_18

[44] Parmar, C.P., Saiyed, S.L. and Vora, K.S., 2020. Health System Preparedness for Screening of Cervical Cancer: Situational Analysis in Tribal District of Gujarat State,

India. *National Journal of Community Medicine*, *11*(02), pp.57-63. DOI: 10.5455/njcm.20190408061631

[45] Intahphuak, S., Nambunmee, K. and Kuipiaphum, P., 2021. Factors influence on PAP test screening among Lahu hill tribe women in remote area Thailand. *Asian Pacific Journal of Cancer Prevention: APJCP*, *22*(7), pp. 2243-49. DOI: 10.31557/APJCP.2021.22.7.2243.

[46] Kritpetcharat, O., Wutichouy, W., Sirijaichingkul, S. and Kritpetcharat, P., 2012. Comparison of Pap Smear screening results between Akha hill tribe and urban women in Chiang Rai province, Thailand. *Asian Pacific Journal of Cancer Prevention*, *13*(11), pp.5501-5504. DOI: 10.7314/apjcp.2012.13.11.5501.

[47] Wongwatcharanukul, L., Promthet, S., Bradshaw, P., Jirapornkul, C. and Tungsrithong, N., 2014. Factors affecting cervical cancer screening uptake by Hmong hilltribe women in Thailand. *Asian Pacific Journal of Cancer Prevention*, *15*(8), pp.3753-3756.. DOI: 10.7314/apjcp.2014.15.8.3753.

[48] Mutambara, J., Mutandwa, P., Mahapa, M., Chirasha, V., Nkiwane, S. and Shangahaidonhi, T., 2017. Knowledge, attitudes and practices of cervical cancer screening among women who attend traditional churches in Zimbabwe. *Journal of Cancer Research and Practice*, *4*(2), pp.53-58.. DOI:10.1016/j.jcrpr.2017.02.001

[49] Kaneko, N., 2018. Factors associated with cervical cancer screening among young unmarried Japanese women: results from an internet-based survey. *BMC women's health*, *18*, pp.1-9. DOI: 10.1186/s12905-018-0623-z

[50] Jradi, H. and Bawazir, A., 2019. Knowledge, attitudes, and practices among Saudi women regarding cervical cancer, human papillomavirus (HPV) and corresponding vaccine. *Vaccine*, *37*(3), pp.530-537. DOI: 10.1016/j.vaccine.2018.11.065.

[51] Waller, J., Bartoszek, M., Marlow, L. and Wardle, J., 2009. Barriers to cervical cancer screening attendance in England: a population-based survey. *Journal of medical screening*, *16*(4), pp.199-204. DOI: 10.1258/jms.2009.009073.

[52] Elfström, K.M., Arnheim-Dahlström, L., von Karsa, L. and Dillner, J., 2015. Cervical cancer screening in Europe: quality assurance and organisation of programmes. *European Journal of Cancer*, *51*(8), pp.950-968. DOI: 10.1016/j.ejca.2015.03.008

[53] Anttila, A. and Nieminen, P., 2007. Cervical cancer screening programme in Finland with an example on implementing alternative screening methods. *Collegium antropologicum*, *31*(2), pp.17-22.

[54] Canfell, K., Sitas, F. and Beral, V., 2006. Cervical cancer in Australia and the United Kingdom: comparison of screening policy and uptake, and cancer incidence and mortality. *Medical Journal of Australia*, *185*(9), pp.482-486. DOI: 10.5694/j.1326-5377. 2006.tb00661. x.

[55] Creighton, P., Lew, J.B., Clements, M., Smith, M., Howard, K., Dyer, S., Lord, S. and Canfell, K., 2010. Cervical cancer screening in Australia: modelled evaluation of the impact of changing the recommended interval from two to three years. *BMC public health*, *10*, pp.1-14. DOI: 10.1186/1471-2458-10-734

[56] Elazab, M., Ali, O., Ramadan, M.C., Hassan, M., Aljedaani, H. and Gardner, F., 2021. The prevalence of human papilloma virus (hpv) among egyptian women and its impact: an observational study. *Open Journal of Obstetrics and Gynecology*, *11*(7), pp.879-884. DOI: 10.4236/ojog.2021.117082

[57] Boselli, F., De Martis, S., Rivasi, F., Toni, A., Abbiati, R. and Chiossi, G., 2000. The Italian experience of a Pap test and speculoscopy based screening programme. *Journal of Medical Screening*, *7*(3), pp.160-162. DOI: 10.1136/jms. 7.3.160

[58] PR Newswire, 2021. *Israeli FemTech Company MobileODT, Engaged in Large Scale Government Cervical Cancer Screening Project*. viewed 22 April 2024, (https://www.prnewswire.com/news-releases/israeli-femtech-company-mobileodt-engaged-in-large-scale-government-cervical-cancer-screening-project-301256186.html /).

[59] Mobileodt.com, 2018. *Cervical cancer screening in China: MobileODT takes part in the largest ever self-swab HPV study*, viewed 22 April 2024 (https://www.mobileodt.com/ blog/cervical-cancer-screening-in-china-largest-ever-self-swab-hpv-study/)

[60] Mobileodt.com, 2017. *Statistics on Clinical Activities and Practices of Cervical Cancer Clinics in Kenya*. viewed 22 April 2024 (https://www.mobileodt.com/ medical-research/clinical-activities-cervical-cancer-screening-camps-stationary-clinics-kenya/)

[61] Peterson, C.W., Rose, D., Mink, J. and Levitz, D., 2016. Real-time monitoring and evaluation of a visual-based cervical cancer screening program using a decision support job aid. *Diagnostics*, *6*(2), p.20. DOI: 10.3390/diagnostics6020020

[62] Mobileodt.com. *MobileODT*, viewed 22 April 2024 (https://www.mobileodt.com/)

[63] Xue, Z., Novetsky, A.P., Einstein, M.H., Marcus, J.Z., Befano, B., Guo, P., Demarco, M., Wentzensen, N., Long, L.R., Schiffman, M. and Antani, S., 2020. A demonstration of automated visual evaluation of cervical images taken with a smartphone camera. *International Journal of Cancer*, *147*(9), pp.2416-2423.. DOI: 10.1002/ijc.33029

[64] mobileodt.com. *Enhanced visual assessment system eva System–Software Guide*. viewed 22 April 2024 (https://portal.mobileodt.com/Help/EVA-Hardware-Guide/)

[65] El Meslouhi, O., Kardouchi, M., Allali, H., Gadi, T. and Benkaddour, Y.A., 2011. Automatic detection and inpainting of specular reflections for colposcopic images. *Central European Journal of Computer Science*, *1*, pp.341-354. DOI: 10.2478/s13537-011-0020-2

[66] Kaggle.com. *Intel & MobileODT Cervical Cancer Screening*. viewed 22 April 2024 (https://www.kaggle.com/c/intel-mobileodt-cervical-cancer-screening/data)

[67] Akbari, M., Mohrekesh, M., Najariani, K., Karimi, N., Samavi, S. and Soroushmehr, S.R., 2018. Adaptive specular reflection detection and inpainting in colonoscopy video frames. In *2018 25th IEEE international conference on image processing (ICIP)* (pp. 3134-3138). IEEE. DOI: 10.1109/ICIP.2018.8451699

[68] Nie, C., Xu, C., Li, Z., Chu, L. and Hu, Y., 2023. Specular reflections detection and removal for endoscopic images based on brightness classification. *Sensors*, *23*(2), p.974. DOI: 10.3390/s23020974

[69] Yu, B., Chen, W., Zhong, Q. and Zhang, H., 2021. Specular highlight detection based on color distribution for endoscopic images. *Frontiers in Physics*, *8*, p.616930. DOI: 10.3389/fphy.2020.616930.

[70] Wang, X., Li, P., Yongzhao, D.U., Lv, Y. and Chen, Y., 2019. Detection and inpainting of specular reflection in colposcopic images with exemplar-based method. In *2019 IEEE 13th International Conference on Anti-counterfeiting, Security, and Identification (ASID)* (pp. 90-94). IEEE., DOI: 10.1109/ICASID.2019.8925202.

[71] Asif, M., Song, H., Chen, L., Yang, J. and Frangi, A.F., 2021. Intrinsic layer based automatic specular reflection detection in endoscopic images. *Computers in Biology and Medicine*, *128*, p.104106. DOI: 10.1016/j.compbiomed.2020.104106.

[72] Kudva, V., Prasad, K. and Guruvare, S., 2017. Detection of specular reflection and segmentation of cervix region in uterine cervix images for cervical cancer screening. IRBM 38: 281–291. DOI: 10.1016/j.irbm.2017.08.003.

[73] Yue, Z., Ding, S., Li, X., Yang, S. and Zhang, Y., 2021. Automatic acetowhite lesion segmentation via specular reflection removal and deep attention network. *IEEE Journal of Biomedical and Health Informatics*, *25*(9), pp.3529-3540. DOI: 10.1109/JBHI.2021.3064366

[74] Gao, Y., Yang, J., Ma, S., Ai, D., Lin, T., Tang, S. and Wang, Y., 2017. Dynamic searching and classification for highlight removal on endoscopic image. *Procedia Computer Science*, *107*, pp.762-767. DOI: 10.1016/j.procs.2017.03.161

[75] Li, R., Pan, J., Si, Y., Yan, B., Hu, Y. and Qin, H., 2019. Specular reflections removal for endoscopic image sequences with adaptive-RPCA decomposition. *IEEE transactions on medical imaging*, *39*(2), pp.328-340. DOI: 10.1109/TMI.2019.2926501

[76] Wang, X., Li, P., Lv, Y., Xue, H., Xu, T., Du, Y. and Liu, P., 2021. Integration of global and local features for specular reflection inpainting in colposcopic images. *Journal of Healthcare Engineering*, *2021*, pp. 1-11. DOI: 10.1155/2021/5401308.

[77] Oak, P. and Iyer, B., 2020. Specular reflection detection and substitution: A key for accurate medical image analysis. In *ICCCE 2019: Proceedings of the 2nd International Conference on Communications and Cyber Physical Engineering* (pp. 223-241). Springer Singapore. DOI: 10.1007/978-981-13-8715-9_28

[78] Shen, D.F., Guo, J.J., Lin, G.S. and Lin, J.Y., 2020. Content-aware specular reflection suppression based on adaptive image inpainting and neural network for endoscopic images. *Computer methods and programs in biomedicine*, *192*, p.105414. DOI: 10.1016/j.cmpb.2020.105414

[79] Das, A. and Choudhury, A., 2017. A novel humanitarian technology for early detection of cervical neoplasia: ROI extraction and SR detection. In *2017 IEEE Region 10 Humanitarian Technology Conference (R10-HTC)* (pp. 457-460). IEEE. DOI: 10.1109/R10-HTC.2017.8288998

[80] Bidokh, E. and Hassanpour, H., 2023. Enhancing Wireless Capsule Endoscopy images from intense illumination specular reflections using the homomorphic filter. *Biomedical Signal Processing and Control*, *84*, p.104723. DOI: 10.1016/j.bspc.2023.104723.

[81] Jha, D., Riegler, M.A., Johansen, D., Halvorsen, P. and Johansen, H.D., 2020. Doubleu-net: A deep convolutional neural network for medical image segmentation. In *2020 IEEE 33rd International symposium on computer-based medical systems (CBMS)* (pp. 558-564). IEEE. DOI: 10.1109/CBMS49503.2020.00111

[82] Zhou, Z., Rahman Siddiquee, M.M., Tajbakhsh, N. and Liang, J., 2018. Unet++: A nested u-net architecture for medical image segmentation. In *Deep Learning in Medical Image Analysis and Multimodal Learning for Clinical Decision Support: 4th International Workshop, DLMIA 2018, and 8th International Workshop, ML-CDS 2018, Held in Conjunction with MICCAI 2018, Granada, Spain, September 20, 2018, Proceedings 4* (pp. 3-11). Springer International Publishing. DOI: 10.1007/978-3-030-00889-5_1

[83] Cao, H., Wang, Y., Chen, J., Jiang, D., Zhang, X., Tian, Q. and Wang, M., 2022, October. Swin-unet: Unet-like pure transformer for medical image segmentation. In *European conference on computer vision* (pp. 205-218). Cham: Springer Nature Switzerland. DOI: 10.1007/978-3-031-25066-8_9

[84] Zhang, Y., Lai, H. and Yang, W., 2021. Cascade UNet and CH-UNet for thyroid nodule segmentation and benign and malignant classification. In *Segmentation, Classification, and Registration of Multi-modality Medical Imaging Data: MICCAI 2020 Challenges, ABCs 2020, L2R 2020, TN-SCUI 2020, Held in Conjunction with MICCAI 2020, Lima, Peru, October 4–8, 2020, Proceedings 23* (pp. 129-134). Springer International Publishing. DOI: 10.1007/978-3-030-71827-5_17

[85] Zhou, Y., Huang, W., Dong, P., Xia, Y. and Wang, S., 2019. D-UNet: a dimension-fusion U shape network for chronic stroke lesion segmentation. *IEEE/ACM transactions on computational biology and bioinformatics*, *18*(3), pp.940-950. DOI: 10.1109/TCBB.2019.2939522

[86] Park, J., Yang, H., Roh, H.J., Jung, W. and Jang, G.J., 2022. Encoder-weighted W-Net for unsupervised segmentation of cervix region in colposcopy images. *Cancers*, *14*(14), p.3400. DOI: 10.3390/cancers14143400

[87] Huang, H., Lin, L., Tong, R., Hu, H., Zhang, Q., Iwamoto, Y., Han, X., Chen, Y.W. and Wu, J., 2020. Unet 3+: A full-scale connected unet for medical image segmentation. In *ICASSP 2020-2020 IEEE international conference on acoustics, speech and signal processing (ICASSP)* (pp. 1055-1059). IEEE. DOI: 10.1109/ICASSP40776.2020.9053405

[88] Niu, H., Lin, Z., Zhang, X. and Jia, T., 2022, May. Image Segmentation for pneumothorax disease Based on based on Nested Unet Model. In *2022 3rd International Conference on Computer Vision, Image and Deep Learning & International Conference on Computer Engineering and Applications (CVIDL & ICCEA)* (pp. 756-759). IEEE. DOI: **10.1109/CVIDLICCEA56201.2022.9824606**

[89] Shinohara, T., Murakami, K. and Matsumura, N., 2023. Diagnosis assistance in colposcopy by segmenting acetowhite epithelium using U-net with images before and after acetic acid solution application. *Diagnostics*, *13*(9), p.1596. DOI: **10.3390/diagnostics13091596**

[90] Yu, H., Fan, Y., Ma, H., Zhang, H., Cao, C., Yu, X., Sun, J., Cao, Y. and Liu, Y., 2022. Segmentation of the cervical lesion region in colposcopic images based on deep learning. *Frontiers in Oncology*, *12*, p.952847. DOI: 10.3389/fonc.2022.952847

[91] Liu, G., Reda, F.A., Shih, K.J., Wang, T.C., Tao, A. and Catanzaro, B., 2018. Image inpainting for irregular holes using partial convolutions. In *Proceedings of the European conference on computer vision (ECCV)* (pp. 85-100). DOI: 10.1007/978-3-030-01252-6_6.

[92] Patel H., Kulkarni A., Sahni S., and Vyas U., "Image Inpainting using Partial Convolution," arXiv Preprint, arXiv:2108.08791v1, 2021.

[93] Mohite, T.A. and Phadke, G.S., 2020. Image inpainting with contextual attention and partial convolution. In *2020 International Conference on Artificial Intelligence and Signal Processing (AISP)* (pp. 1-6). IEEE. DOI:10.1109/AISP48273.2020.9073008.

[94] Kaur, A., Raj, A., Jayanthi, N. and Indu, S., 2020. Inpainting of irregular holes in a manuscript using unet and partial convolution. In *2020 Second International Conference on Inventive Research in Computing Applications (ICIRCA)* (pp. 778-784). IEEE. DOI:10.1109/ICIRCA48905.2020.9182917.

[95] Chen, M., Zhao, X. and Xu, D., 2019. Image inpainting for digital Dunhuang murals using partial convolutions and sliding window method. In *Journal of Physics: Conference Series* (Vol. 1302, No. 3, p. 032040). IOP Publishing. DOI:10.1088/1742- 6596/1302/3/032040.

[96] Yan, S. and Zhang, X., 2022. PCNet: Partial convolution attention mechanism for image inpainting. *International Journal of Computers and Applications*, *44*(8), pp.738-745.. 10.1080/08839514.2021.1988441.

[97] Kang, J., Lee, S., Heo, S. and Lee, S., 2020. Image inpainting using weighted mask convolution. In *2020 Asia-Pacific Signal and Information Processing Association Annual Summit and Conference (APSIPA ASC)* (pp. 1262-1267). IEEE..

[98] Cai, N., Su, Z., Lin, Z., Wang, H., Yang, Z. and Ling, B.W.K., 2017. Blind inpainting using the fully convolutional neural network. *The Visual Computer*, *33*, pp.249-261. DOI: 10.1007/s00371-015-1190-z.

[99] Liu, Y., Pan, J. and Su, Z., 2019. Deep blind image inpainting. In *Intelligence Science and Big Data Engineering. Visual Data Engineering: 9th International Conference, IScIDE 2019, Nanjing, China, October 17–20, 2019, Proceedings, Part I 9* (pp. 128-141). Springer International Publishing. DOI: 10.1007/978-3- 030-36189-1_11.

[100] Wang, Y., Chen, Y.C., Tao, X. and Jia, J., 2020. Vcnet: A robust approach to blind image inpainting. In *Computer Vision–ECCV 2020: 16th European Conference, Glasgow, UK, August 23–28, 2020, Proceedings, Part XXV 16* (pp. 752-768). Springer International Publishing. DOI: 10.1007/978-3-030-58595- 2_45.

[101] Schmalfuss, J., Scheurer, E., Zhao, H., Karantzas, N., Bruhn, A. and Labate, D., 2023. Blind image inpainting with sparse directional filter dictionaries for lightweight CNNs. *Journal of Mathematical Imaging and Vision*, *65*(2), pp.323-339. DOI: 10.1007/s10851-022-01119-6

[102] Yu, J., Lin, Z., Yang, J., Shen, X., Lu, X. and Huang, T.S., 2019. Free-form image inpainting with gated convolution. In *Proceedings of the IEEE/CVF international conference on computer vision* (pp. 4471-4480). DOI:10.1109/ICCV.2019.00457.

[103] Dai, P., Ji, S. and Zhang, Y., 2020. Gated convolutional networks for cloud removal from bi-temporal remote sensing images. *Remote Sensing*, *12*(20), p.3427. DOI: 10.3390/rs12203427.

[104] Chang, Y.L., Liu, Z.Y., Lee, K.Y. and Hsu, W., 2019. Free-form video inpainting with 3d gated convolution and temporal patch GAN. In *Proceedings of the IEEE/CVF International Conference on Computer Vision* (pp. 9066 - 9075). DOI: 10.48550/arXiv.1904.10247.

[105] Wei, R. and Wu, Y., 2022. Image Inpainting via Context Discriminator and U-Net. *Mathematical Problems in Engineering*, *2022(1)*, pp.1 - 12. DOI:10.1155/2022/7328045.

[106] Yan, Z., Li, X., Li, M., Zuo, W. and Shan, S., 2018. Shift-net: Image inpainting via deep feature rearrangement. In *Proceedings of the European conference on computer vision (ECCV)* (pp. 1-17). DOI: 10.1007/978-3-030-01264-91.

[107] Zhou, X., Dai, T., Jiang, Y. and Xia, S.T., 2021. Bishift-net for image inpainting. In *ICASSP 2021-2021 IEEE International Conference on Acoustics, Speech and Signal Processing (ICASSP)* (pp. 2470-2474). IEEE. DOI:10.1109/ICASSP39 728.2021.9413380.

[108] Hong, X., Xiong, P., Ji, R. and Fan, H., 2019. Deep fusion network for image completion. In *Proceedings of the 27th ACM international conference on multimedia* (pp. 2033-2042). DOI: 10.1145/3343031.3351002.

[109] Zeng, Y., Fu, J., Chao, H. and Guo, B., 2019. Learning pyramid-context encoder network for high-quality image inpainting. In *Proceedings of the IEEE/CVF conference on computer vision and pattern recognition* (pp. 1486-1494). DOI: 10.1109/CVPR.2019.00158. 2019.

[110] Salem, N.M., Mahdi, H.M. and Abbas, H.M., 2019. Random-shaped image inpainting using dilated convolution. *Int. J. Eng. Adv. Technol. IJEAT*, *8*, pp.641-647. DOI: 10.35940/ijeat.F8089.088619.

[111] Prabhu, R., Yu, X., Wang, Z., Liu, D. and Jiang, A., 2019. U-finger: Multi-scale dilated convolutional network for fingerprint image denoising and inpainting. In *Inpainting and Denoising Challenges* (pp. 45-50). Springer International Publishing.DOI: 10.1007/978-3-030-25614- 2_3.

[112] Pimkin, A., Samoylenko, A., Antipina, N., Ovechkina, A., Golanov, A., Dalechina, A. and Belyaev, M., 2020. Multidomain CT metal artifacts reduction using partial convolution based inpainting. In *2020 International Joint Conference on Neural Networks (IJCNN)* (pp. 1-6). IEEE. DOI: 10.1109/IJCNN48605.2020.9206625

[113] Manjón, J.V., Romero, J.E., Vivo-Hernando, R., Rubio, G., Aparici, F., de La Iglesia-Vaya, M., Tourdias, T. and Coupé, P., 2020. Blind MRI brain lesion inpainting using deep learning. In *Simulation and Synthesis in Medical Imaging: 5th International Workshop, SASHIMI 2020, Held in Conjunction with MICCAI 2020, Lima, Peru, October 4, 2020, Proceedings 5* (pp. 41-49). Springer International Publishing. DOI:10.1007/978-3-030-59520- 3_5

[114] Zhou, Q., Zhu, W., Li, F., Yuan, M., Zheng, L. and Liu, X., 2022. Transfer learning of the ResNet-18 and DenseNet-121 model used to diagnose intracranial hemorrhage in CT scanning. *Current Pharmaceutical Design*, *28*(4), pp.287-295. DOI: 10.2174/1381612827666211213143357

[115] Kumar, K.A., Prasad, A.Y. and Metan, J., 2022. A hybrid deep CNN-Cov-19-Res-Net Transfer learning architype for an enhanced Brain tumor Detection and Classification scheme in medical image processing. *Biomedical Signal Processing and Control*, *76*, p.103631. DOI: 10.1016/j.bspc.2022.103631

[116] Huang, Z., Zhu, X., Ding, M. and Zhang, X., 2020. Medical image classification using a light-weighted hybrid neural network based on PCANet and DenseNet. *Ieee Access*, *8*, pp.24697-24712. DOI: 10.1109/ACCESS.2020.2971225.

[117] Sarwinda, D., Paradisa, R.H., Bustamam, A. and Anggia, P., 2021. Deep learning in image classification using residual network (ResNet) variants for detection of colorectal cancer. *Procedia Computer Science*, *179*, pp.423-431. DOI: 10.1016/j.procs.2021.01.025.

[118] Pattanaik, R.K., Mishra, S., Siddique, M., Gopikrishna, T. and Satapathy, S., 2022. Breast cancer classification from mammogram images using extreme learning machine-based DenseNet121 model. *Journal of Sensors*, *2022*. DOI: 10.1155/2022/2731364

[119] Chandran, V., Sumithra, M.G., Karthick, A., George, T., Deivakani, M., Elakkiya, B., Subramaniam, U. and Manoharan, S., 2021. Diagnosis of cervical cancer based on ensemble deep learning network using colposcopy images. *BioMed Research International*, *2021*. DOI: 10.1155/2021/5584004

[120] Nayak, D.R., Padhy, N., Mallick, P.K., Zymbler, M. and Kumar, S., 2022. Brain Tumor Classification Using Dense Efficient-Net. Axioms 2022, 11, 34. *Mathematical Fuzzy Logic in the Emerging Fields of Engineering, Finance, and Computer Sciences*, *151*. DOI: 10.3390/axioms11010034

[121] Phine, S., 2023. Pneumonia classification using deep learning vgg19 model. In *2023 IEEE Conference on Computer Applications (ICCA)* (pp. 67-71). IEEE. DOI: 10.1109/ICCA51723.2023.10181954

[122] Shah, H.A., Saeed, F., Yun, S., Park, J.H., Paul, A. and Kang, J.M., 2022. A robust approach for brain tumor detection in magnetic resonance images using finetuned efficientnet. *Ieee Access*, *10*, pp.65426-65438. DOI: 10.1109/ACCESS.2022. 3184113.

[123] Munien, C. and Viriri, S., 2021. Classification of hematoxylin and eosin-stained breast cancer histology microscopy images using transfer learning with EfficientNets. *Computational Intelligence and Neuroscience*, *2021*.DOI: 10.1155/2021/5580914

[124] Alyafeai, Z. and Ghouti, L., 2020. A fully-automated deep learning pipeline for cervical cancer classification. *Expert Systems with Applications*, *141*, p.112951. DOI: 10.1016/j.eswa.2019.112951

[125] Yoon, K., Seol, J. and Kim, K.G., 2022. Removal of specular reflection using angle adjustment of linear polarized filter in medical imaging diagnosis. *Diagnostics*, *12*(4), p.863. DOI: 10.3390/diagnostics12040863

[126] Suo, J., An, D., Ji, X., Wang, H. and Dai, Q., 2016. Fast and high quality highlight removal from a single image. *IEEE Transactions on Image Processing*, *25*(11), pp.5441-5454. DOI: 10.1109/TIP.2016.2605002

[127] Shelhamer, E., Long, J. and Darrell, T., 2017. Fully convolutional networks for semantic segmentation. *IEEE Trans. Pattern Anal. Mach. Intell.*, *39*(4), pp.640-651. DOI: 10.1109/CVPR.2015.7298965

[128] Badrinarayanan, V., Kendall, A. and Cipolla, R., 2017. Segnet: A deep convolutional encoder-decoder architecture for image segmentation. *IEEE transactions on pattern analysis and machine intelligence*, *39*(12), pp.2481-2495. DOI: 10.1109/TPAMI.2016.2644615

[129] Ronneberger, O., Fischer, P. and Brox, T., 2015. U-net: Convolutional networks for biomedical image segmentation. In *Medical Image Computing and Computer-Assisted Intervention–MICCAI 2015: 18th International Conference, Munich, Germany, October 5-9, 2015, Proceedings, Part III 18* (pp. 234-241). Springer International Publishing. DOI: 10.1007/978-3-319-24574-4_28

[130] Siddique, N., Paheding, S., Elkin, C.P. and Devabhaktuni, V., 2021. U-net and its variants for medical image segmentation: A review of theory and applications. *Ieee Access*, *9*, pp.82031-82057. DOI: 10.1109/ACCESS.2021.3086020.

[131] Paris, S., Kornprobst, P., Tumblin, J. and Durand, F., 2009. Bilateral filtering: Theory and applications. *Foundations and Trends® in Computer Graphics and Vision*, *4*(1), pp.1-73. DOI: 10.1561/0600000020.

[132] Huang, W., Deng, Y., Hui, S. and Wang, J., 2022. Image Inpainting with Bilateral Convolution. *Remote Sensing*, *14*(23), p.6140. DOI: 10.3390/rs14236140.

[133] Huang, G., Liu, Z., Van Der Maaten, L. and Weinberger, K.Q., 2017. Densely connected convolutional networks. In *Proceedings of the IEEE conference on computer vision and pattern recognition* (pp. 4700-4708). DOI: 10.1109/CVPR.2017.243

[134] Liu, S. and Deng, W., 2015, November. Very deep convolutional neural network based image classification using small training sample size. In *2015 3rd IAPR Asian conference on pattern recognition (ACPR)* (pp. 730-734). IEEE.DOI: 10.1109/ACPR.2015.7486599.

[135] Tan, M. and Le, Q., 2019, May. Efficientnet: Rethinking model scaling for convolutional neural networks. In *International conference on machine learning* (pp. 6105-6114). PMLR. DOI: 10.48550/arXiv.1905.11946

[136] Park, J.B., 2004, August. Detection of specular highlights in color images using a new color space transformation. In *2004 IEEE International Conference on Robotics and Biomimetics* (pp. 737-741). IEEE.

[137] Morgand, A. and Tamaazousti, M., 2014, January. Generic and real-time detection of specular reflections in images. In *2014 International conference on computer vision theory and applications (VISAPP)* (Vol. 1, pp. 274-282). IEEE.

[138] Triwijoyoa, B.K. and Adila, A., 2021. Analysis of medical image resizing using bicubic interpolation algorithm. *J. Ilmu Komput*, *14*(2), pp.20-29. DOI: 10.24843/JIK.2021.v14.i01.p03

[139] OSF Home, The HyperKvasir Dataset, viewed 22 April 2024 (https://osf.io/mh9sj/)

[140] Kaggle, esophageal endoscopy images, viewed 22 April 2024 (https://www.kaggle.com/datasets/engnooralmayahi/esophageal-endoscopy-images/)

[141] WHO, IARC Cervical Cancer Image Bank, viewed 22 April 2024 (https://screening.iarc.fr/cervicalimagebank.php/)

[142] Wang, Y., Sun, Z., Liu, C., Peng, W. and Zhang, J., 2016, August. MRI image segmentation by fully convolutional networks. In *2016 IEEE International Conference on Mechatronics and Automation* (pp. 1697-1702). IEEE.

[143] Huang, S.Y., Hsu, W.L., Hsu, R.J. and Liu, D.W., 2022. Fully convolutional network for the semantic segmentation of medical images: A survey. *Diagnostics*, *12*(11), p.2765.

[144] Benedetti, P., Femminella, M. and Reali, G., 2022. Mixed-Sized Biomedical Image Segmentation Based on U-Net Architectures. *Applied Sciences*, *13*(1), p.329.

[145] Müller, D., Soto-Rey, I. and Kramer, F., 2022. Towards a guideline for evaluation metrics in medical image segmentation. *BMC Research Notes*, *15*(1), p.210.

[146] Mique, E. and Malicdem, A., 2020, April. Deep residual u-net based lung image segmentation for lung disease detection. In *IOP conference series: materials science and engineering* (Vol. 803, No. 1, p. 012004). IOP Publishing.

[147] Yin, X.X., Sun, L., Fu, Y., Lu, R. and Zhang, Y., 2022. U-Net-Based medical image segmentation. *Journal of Healthcare Engineering*, *2022*.

[148] Buyssens, P., Daisy, M., Tschumperlé, D. and Lézoray, O., 2015. Exemplar-based inpainting: Technical review and new heuristics for better geometric

reconstructions. *IEEE transactions on image processing*, *24*(6), pp.1809-1824. DOI:10.1109/TIP.2015.2411437.

[149] Liu, G., Shih, K., Wang, T.C., Tao, A. and Catanzaro, B., Nvidia Corp, 2019. *Image in-painting for irregular holes using partial convolutions*. U.S. Patent Application 16/360,895.

[150] Isola, P., Zhu, J.Y., Zhou, T. and Efros, A.A., 2017. Image-to-image translation with conditional adversarial networks. In *Proceedings of the IEEE conference on computer vision and pattern recognition* (pp. 1125-1134).

[151] Wang, Y., Tao, X., Qi, X., Shen, X. and Jia, J., 2018. Image inpainting via generative multi-column convolutional neural networks. *Advances in neural information processing systems*, *31*.

[152] Salem, N.M., Mahdi, H.M. and Abbas, H.M., 2019. Random-shaped image inpainting using dilated convolution. *Int. J. Eng. Adv. Technol. IJEAT*, *8*, pp.641-647. DOI: 10.35940/ijeat.F8089.088619

[153] Elharrouss, O., Almaadeed, N., Al-Maadeed, S. and Akbari, Y., 2020. Image inpainting: A review. *Neural Processing Letters*, *51*, pp.2007-2028. DOI: 10.1007/s11063-019-10163-0.

[154] Hadhoud, M.M., Moustafa, K.A. and Shenoda, S.Z., 2008. Digital images inpainting using modified convolution based method. *International journal of signal processing, image processing and pattern recognition*, *1*(1), pp.1-10.

[155] Rana, M.S., Satter, A.Z., Wahid, Z. and Bhuiyan, T., 2017, September. Inpainting on Digital Images Using Convolution based Method: A Comparison Study. In *Proceedings of the 2017 International Conference on Biomedical Engineering and Bioinformatics* (pp. 38-42).

[156] Paris, S., Kornprobst, P., Tumblin, J. and Durand, F., 2009. Bilateral filtering: Theory and applications. *Foundations and Trends® in Computer Graphics and Vision*, *4*(1), pp.1-73.

[157] Hung, K.W. and Siu, W.C., 2012, January. Real-time interpolation using bilateral filter for image zoom or video up-scaling/transcoding. In *2012 IEEE International Conference on Consumer Electronics (ICCE)* (pp. 67-68). IEEE. DOI: 10.1109/ICCE.2012.6161740.

[158] Liu, L. and Liu, Y., 2022. Load image inpainting: An improved U-Net based load missing data recovery method. *Applied Energy*, *327*, p.119988.

[159] Zhang, L. and Chang, M., 2021. An image inpainting method for object removal based on difference degree constraint. *Multimedia Tools and Applications*, *80*, pp.4607-4626.

[160] Chen, C., Nishio, T., Bennis, M. and Park, J., 2022. Rf-inpainter: Multimodal image inpainting based on vision and radio signals. *IEEE Access*, *10*, pp.110689-110700.

[161] Xie, K., Gao, L., Lu, Z., Li, C., Xi, Q., Zhang, F., Sun, J., Lin, T., Sui, J. and Ni, X., 2022. Inpainting the metal artifact region in MRI images by using generative adversarial networks with gated convolution. *Medical Physics*, *49*(10), pp.6424-6438.

[162] Kaggle, Places-2_MIT_Dataset, viewed 22 April 2024 , (https://www.kaggle.com/datasets/nickj26/places2-mitdataset?select=train_256_places365standard/)

[163] QMUL-OpenLogo, *Open Logo Detection Challenge,* viewed 22 April 2024, (https://hangsu0730.github.io/qmul-openlogo/)

[164] Kaggle, Understanding Clouds from Satellite Images, viewed 22 April 2024, (https://www.kaggle.com/competitions/understanding_cloud_organization/data?select=train_images/)

[165] Uddin, S.N. and Jung, Y.J., 2020. Global and local attention-based free-form image inpainting. *Sensors*, *20*(11), p.3204.

[166] Chen, Y., Xia, R., Yang, K. and Zou, K., 2024. MFMAM: Image inpainting via multi-scale feature module with attention module. *Computer Vision and Image Understanding*, *238*, p.103883.

[167] Zhang, R., Quan, W., Wu, B., Li, Z. and Yan, D.M., 2020, October. Pixel-wise dense detector for image inpainting. In *Computer Graphics Forum* (Vol. 39, No. 7, pp. 471-482).

PUBLICATIONS

Patent Publication

1. Subashini, P., Dhivyaprabha, T.T., **Jennyfer Susan, M.B**. Cervical Cancer Self-Test Kit , Application No.-202241021066,May 2022.

Book Publication

1. Subashini, P., Dhivyaprabha, T.T., **Jennyfer Susan, M.B**. (2023). Machine Learning Using Google Colab – for Chemistry and Biochemistry Applications, *Notion Press*. ISBN: 9798889239963.

Chapter Publications

1. Subashini, P., Dhivyaprabha, T.T., Krishnaveni, M., **Jennyfer Susan, M.B**. (2023). Smart Intelligent System for Cervix Cancer Image Classification Using Google Cloud Platform. In: Ahad, M.A., Casalino, G., Bhushan, B. (eds***) Enabling Technologies for Effective Planning and Management in Sustainable Smart Cities.*** Springer, Cham, PP. 245-281. https://doi.org/10.1007/978-3-031-22922-0_10.
2. **Jennyfer Susan, M.B**., Subashini, P., Krishnaveni, M. (2023). Artificial Intelligence of Things for Smart Health Care Development – An Experimental Review, In P. Swarnalatha & S. Prabu (Eds.), *Handbook of Research on Deep Learning Techniques for Cloud-Based Industrial IoT* (pp. 29-60). IGI Global. https://doi.org/10.4018/978-1-6684-8098-4.ch003**.**

Conference Publication

1. **M.B. Jennyfer Susan**. and P. Subashini. (2019). "Design and Development of Webportal for Cervical cancer Diagnosis using MobileODT Images, *2019 IEEE International Smart Cities Conference (ISC2)*, Casablanca, Morocco, pp. 118-121. DOI: 10.1109/ISC246665.2019.9071683. (**IEEE**)
2. **M.B. Jennyfer Susan**. and P. Subashini. (2021) "Specular Reflection Detection on Digital Images – A Review," *Artificial Intelligence and Soft Computing (ICAISC)*, Karnataka, pp. 506-516. ISBN: 978-93-88929-53-0. (**Offline Proceeding**)

3. **M.B. Jennyfer Susan**. and P. Subashini, "Detection of Specular Reflection on Smart Colposcopy Image Using Fine-Tuned U-Net Model,"*Engineering, Science, and Sustainability Advancements in Technology and Techniques*, Proceeding of *International Sustainability Conference*, Edited By Dimitrios A Karras, Sai Kiran Oruganti, Sudeshna Ray, pp. 163-168, ISBN: 9781032484235 (**CRC publishers**).

4. TT, Dhivyaprabha, **M.B. Jennyfer Susan,** P. Subashini, Pooja Sri Saraswathi, R. VijayaBhanu "An Intelligent Model to Forecast Blood Brain Barrier Permeability using Graph Neural Networks," Third International Conference on Advances in Physical Sciences and Materials, (**Accepted - Indexed in Scopus and CPCI(WOS) – AIP roceedings**).

5. TT, Dhivyaprabha**, M.B. Jennyfer Susan,** P. Lalitha,P. Subashini, Kamalini D, and R. VijayaBhanu "Predicting Ethylene Production in Oxidative Coupling of Methane: A Machine Learning Approach," Third International Conference on Advances in Physical Sciences and Materials, (**Accepted - Indexed in Scopus and CPCI(WOS) – AIP Proceedings**).

Journal Publication

1. **M.B. Jennifer Susan**, P. Subashini, and M. Krishnaveni. (2022). Comparison of various deep learning inpainting methods in smart colposcopy images, *International Journal of Computational Intelligence Studies*, Vol.11, No.1, pp. 53-72. DOI: 10.1504/IJCISTUDIES.2022.123347 – (**UGC CARE**).

2. **M.B. Jennyfer Susan**, P. Subashini. (2023). Improvising Grading of Cervical Cancer using Quality Assessments method in Smart Colposcopy Images, *Measurement Sensors*, Vol. 27, No. 3, pp. 1-11. DOI: 10.1016/j.measen. 2023. 100788. **(SCOPUS)**

3. **M.B. Jennyfer Susan**, P. Subashini. (2023). Deep Learning Inpainting Model on Digital and Medical Images – A Review**,** *International Arab Journal of Information Technology*, Vol. 20, No. 6, pp. 919-936. DOI: 10.34028/iajit/20/6/9 (**SCI and SCOPUS)**

4. **M.B. Jennyfer Susan**, P. Subashini, Krishnaveni M, Indhumathi T (2023). *Detection of Specular Reflection from Smart Colposcopy Image using RGB color space and Convolutional Neural Network*, *International Journal of Engineering Trends and Technology*, Vol. 71, No. 10, pp.29-38, DOI: 10.14445/22315381/ IJETT-V71I10P204 (**SCOPUS)**

Avinashilingam Institute for HomeScience and Higher Education for Women
(Deemed to be University Estd. u/s 3 of UGC Act 1956, Category 'A' by MHRD
Re-accredited with A++ Grade by NAAC. CGPA 3.65/4, Category I by UGC
Coimbatore - 641 043, Tamil Nadu, India

Appendix L2

(Item No 5 of Check List) Details of Research Publications

S.No	Article	Journal	Other Details Vol/No/Page No/ Year	Published in UGC-CARE / Scopus Indexed/ Web of Science
1	Comparison of various deep learning inpainting method in Smart colposcopy Images.	International Journal of computational Intelligence Studies.	Vol. 11, No. 1 PP: 53-72 2022	UGC care Gp. I
2	Improvising grading of cervical cancer using Quality Assessments method in Smart colposcopy Images.	Measurement Sensors.	Vol. 27, No. 3 PP. 1-11 June 2023	Scopus.

*Proof of list of Journals from Internet to be attached along with copies of reprints.

Scholar : Jennyfer Susan. M. B

Supervisor : Dr. P. Subashini.

Checked By:

HoD/Dean of Respective School

The details of publication of the scholar Miss. Jennyfer Susan, M.B. (19PHCSF008) are as follows:

1. International Journal of Computational Intelligence studies- is indexed and active in UGC care List Group I from June 2019 to present. The scholar published her paper in Vol. 11, ~~[illegible]~~ No. 1, 2022 Pg. No. 53-72.

2. measurement: Sensors – is indexed and active in Scopus from 2019 to present. The scholar published her article in Vol. 27, No. 3, June, 2023 Pg. 1-11.

J. [signature]

~~12.10.23~~
~~06.12.23~~
02.01.24

Comparison of various deep learning inpainting methods in smart colposcopy images

M.B. Jennyfer Susan*, P. Subashini and M. Krishnaveni

Department of Computer Science,
Avinashilingam Institute for Home Science and
Higher Education for Women,
Coimbatore, India
Email: 19phcsf008@avinuty.ac.in
Email: subashini_cs@avinuty.ac.in
Email: krishnaveni_cs@avinuty.ac.in
*Corresponding author

Abstract: The specular reflection appears as white area on the cervical images that covers certain region of the images. It affects the quality of the cervical images causing difficulty for the physician to analyse the smart colposcopy images. In this paper, specular reflection is detected and removed from the cervical images, and these removed pixels are refilled using the inpainting methods. To fill the removed pixels, the deep learning inpainting algorithms like partial convolutional neural network, generative multicolumn convolutional neural network, and the dilated convolutional neural network to were used to get the complete and enhanced cervical images. The enhanced images are considered for lesion identification using the Bayes classifier. Based on the analysis, the partial convolution inpainting method gives higher quality with the PSNR value of 48.25 dB and SSIM value of 0.984. The enhanced images using the partial inpainting method identify the neoplasm with an accuracy of 98%.

Keywords: smart colposcope; specular reflection; lesion detection; convolutional neural network; inpainting; Bayes classifier.

Reference to this paper should be made as follows: Jennyfer Susan, M.B., Subashini, P. and Krishnaveni, M. (2022) 'Comparison of various deep learning inpainting methods in smart colposcopy images', *Int. J. Computational Intelligence Studies*, Vol. 11, No. 1, pp.53–72.

Biographical notes: M.B. Jennyfer Susan is currently pursuing her PhD at the Center for Machine learning and Intelligence at Avinashilingam Institute for Home Science and Higher Education for Women, Tamil Nadu, India. She received her MSc in Computer Science at Bharathiar University, Tamil Nadu, India in 2018. Her research interest includes computer vision with deep learning, and artificial intelligence.

P. Subashini is working for the Department of Computer Science, Avinashilingam University, Tamil Nadu India from 1994. She is a coordinator of the Centre for Machine Learning and Intelligence sanctioned by Department of Science and Technology. Her research has spanned various disciplines like image analysis, pattern recognition, neural networks, and computational intelligence. She authored and co-authored four books, four book chapters, one monograph, and 145 research papers both at international and national levels.

She sponsored ten research projects worth more than 2.54 crores from government funding agencies. She extended her contribution towards various international collaborations with universities from the USA, Germany, and Morocco.

M. Krishnaveni is an Assistant Professor of Department of Computer Science, Avinashilingam University for Women, Coimbatore, Tamil Nadu, India. She has research experience under defence projects and worked on disciplines like IoT, image processing, speech processing, data mining, and computational intelligence. She has published four books, six book chapters, one monograph and 86 research papers in both national and international level. She has research projects under various funding agencies and acts as an active member of centre for machine learning and artificial intelligence and coordinating AI start-up program (Product Development Lab) for the student.

1 Introduction

Cervical cancer is a malignancy that is observed at the lower part of the uterus. It is the fourth most female cancer reported worldwide. Based on Global analysis in the year 2020, (Balasubramaniam et al., 2021) reported that 604,237 women have been diagnosed and 341,843 women are killed due to cervical cancer. On analysing the total death rate, 90% of the women belong to the developing countries to the regions with the lack of prevention measures, screening, and treatment for cervical cancer. In India, cervical cancer has ranked the second most common cancer among women. Based on the statistical analysis, 96,922 new cases and 60,078 deaths were reported due to cervical cancer in the year 2020. Many of the women are from the rural and tribal regions of India. It is due to the lack of awareness and minimum clinical setup for screening women in the rural and tribal regions of India (Reichheld et al., 2020).

Cervical cancer is caused by human papillomavirus (HPV) which is a sexually transmitted infection, and it is prevented by the HPV vaccinations (Wang et al., 2021). Some of the other factors that lead to the cause of cervical cancer are smoking, obesity, early marriage, high intake of miscarriage prevention drugs, and a weak immune system. The cervical cancer symptoms shown are highly unnoticeable which are the cause for the increase of cervical cancer, and it is cured when treated at its initial stage (Gevorg and Hakob, 2013). Regular screening for every six-month helps in the reduction of cervical cancer. There are many screening camps that are provided in the rural and tribal regions of India to reduce the morality rate of cervical cancer. But still, there is a hesitation among women because the cervical cancer screening is a time-consuming process. To overcome the problem, the enhanced visual assessment (EVA) tool has been introduced for the screening the cervical cancer. It is portable and takes less time for screening the cervical cancer with minimum manpower. Smart colposcope helps in capturing the high-quality cervix images with the 16x optical magnification which are taken for analysis of tissue structure and dysplasia detection. During the analysis the quality of the cervical images are affected by noise called secular reflection.

Specular reflection is the white bright pixels that are caused by the light reflection on the captured cervical images (Das et al., 2011). The smart colposcope is connected with the 6,000 K 3W LED light to focus the cervical region with a wire grid polariser for glare reduction on the captured cervical images (MobileODT, 2021). But still some of the cervical images are affected by specular reflection which occurs due to the water content of the tissue bodies that absorb light from the surrounding area and reflect as a specular reflection as shown in Figure 1. The quality of the images gets affected due to the appearance of glare region on the cervical images. To improve the quality of the cervix images, the glare regions should be identified and removed from the images. The removed region on the cervical images should be inpainted using the deep learning algorithm to refill the missing pixels on the cervical images.

Figure 1 The EVA colpo, (a) the smart colposcope (b) the cervix images captured through smart colposcope with the specular reflection (see online version for colours)

(a) (b)

This paper is organised in the following manners. Section 2 analyses the related work of convolutional neural network models and generative models which are used for the removal and inpainting specular reflection regions on the cervical images. Section 3 analyses the proposed methodologies for the detection and removal of specular reflection on the cervical images. The removed regions are inpainted using the deep learning algorithm to improve the quality of the cervical images. The detection of the neoplasm was analysed on the enhanced and non-enhanced cervical images. Section 4 discusses the experimental result obtained using the above analysis and Section 5 is the discussion of the paper. Finally, Section 6 is the conclusion of the paper.

2 Related works

Specular reflection appears as the white intense on the cervical images. It almost appears like the dysplasia region or acetowhite region and covers a certain region with its bright light with its reflection properties. For the detection of specular reflection colour space model is used and for refilling the missing pixels inpainting methods are used. Inpainting is the traditional method highly used in digital images for refilling the missing pixels. During earlier times, many detections and inpainting methods have been proposed for the removal of specular reflection removal but very less method are automated (Gevorg and Hakob, 2013; Arnold et al., 2010). Some of the few methods are automated for inpainting the specular reflection from the cervical images which is captured through smart colposcopy. During recent years, the computer vision along with the deep learning algorithm are highly used for inpainting the missing pixels. The related paper is discussed more in detail in the Table 1.

Table 1 A related paper of this paper

Author	*Algorithm*	*Methodology*	*Result*
Das et al. (2011)	RGB color space, morphological operation and Laplace equation	• Each plane of the RGB color is extracted by logically adding them to detect the white region. • Morphological operation is used to detect the outline of the reflection region. • The detected region is filled by using Laplace's equation.	• This method helps in detecting the white region on the cervix images and refilling them. • It is a pre-processing method to detect the region of interest on the cervix images.
Lange et al. (2005)	RGB colourspace, HSV colourspace, HSI color space Sequential filter, watershed operation and Laplace equation	• The feature value is extracted using the mean and min value of the RGB channel and along with the S value of the HSV color space. • The sequential filters and the watershed operation are used to obtain the maximum position minima • It is a threshold value to detect saturated regions on cervix images. • Laplace's equation along with the modified I value of the HSI colour space to remove the glare portion on the cervix images.	• It is pre-processing method for improvising the quality of the cervix images. • The glare located in the white region with a dark background detects as the entire region belongs to the reflection region and is removed on the cervical images. • The glare region located in the more on one region than the color in the smaller region spreads and affects the quality of certain cervical images.
Pallavi et al. (2011)	RGB color space and histogram value	• The G component from the RGB colourspace is used to extract the feature of the glare region. • The histogram is applied to extract the local minima region for the G component to extract the glare region.	• It is a pre-processing method to improve the quality of cancer detection. • This is applied on the pre acetic, post acetic and post Lugol Iodine images.
Pathak et al. (2016)	Generative adversarial network (GAN) with the encoder-decoder pipeline	• GAN is an unsupervised method for predating missing pixels on the images. • The encoder latent the features of the missing pixels. • It is derived from Alexnet with one stride convolution, feature map, sampling layer and activation function (ReLu). • The decoder predicts the missing pixels on the digital images.	• The proposed method is compared with the context encoder algorithm. • The context encoder fails to generate good resolution images and time consuming for the training algorithm. • The up-sampling method is used to retain the resolution of the images.

Table 1 A related paper of this paper (continued)

Author	*Algorithm*	*Methodology*	*Result*
Iizuka et al. (2019)	Convolutional neural network, dilated convolutional neural network, local context discriminator, and global context discriminator	• It is a pixel based inpainting method. • The dilation neural network increases the speed of feature extraction on digital images. • The local and global context discriminator predicts and fills the missing pixels respectively. • The global context discriminator takes the complete input images, and the local context discriminator completed the small empty portion on the input images.	• The proposed method fixes the low-resolution output images when compared with the context encoder method. • It is used in many digital images to predict the missing region on the digital images.
Demir et al. (2018)	Patch generative adversarial network discriminator network with the global generative adversarial network (G-GAN)	• It is a patch-based inpainting method. • The ResNet is used as a generative network to fill up the large holes in the digital images.	• The proposed method has been highly performed when compared with the existing inpainting method like GLGAN, PGGAN, and NPS algorithms. • It is suitable to refill the large holes in the digital images. • The drawback is that it is not suitable for the random missing pixels.
Jiahui et al. (2019)	Gated convolutional neural network	• It is built with the SN patch GAN. • It is a learnable version of the partial convolutional neural network to validate the feature value. • It is activated with the sigmoid function.	• The proposed is compared with the related paper, in which the proposed network gives higher quality of inpainting images. • It helps in fixing up the random missing pixel, but the resolution of the images gets affected in the digital images.
Huang et al. (2008)	Mean shift clustering and support vector machine	The Gaussian mixture clustering and features are extracted to detect the cancer region on the cervix images	• It is an unsupervised method for cancer detection. • Based on the comparative analysis the accuracy of the proposed method gives high detection. • But in many regions, non-acetowhite regions are also detected as lesion regions.

3 Proposed methodology

This section discusses the algorithm used for detection and removal of specular reflection on the cervical images. After the detection and removal of specular reflection, the removed specular region should be refilled using the neighbouring pixels based on the deep learning inpainting methods. For this refilling method, a comparison of three deep learning inpainting methods is applied to the empty region of the cervical images. It will refill the empty portion of the cervical images with the neighbouring pixel automatically. It acts as an enhancement method to improve the quality of cervical images. The enhanced images are used for dysplasia detection on the cervical images. The methodology of this paper is represented as a block diagram as shown in Figure 2.

Figure 2 Block diagram of the methodology

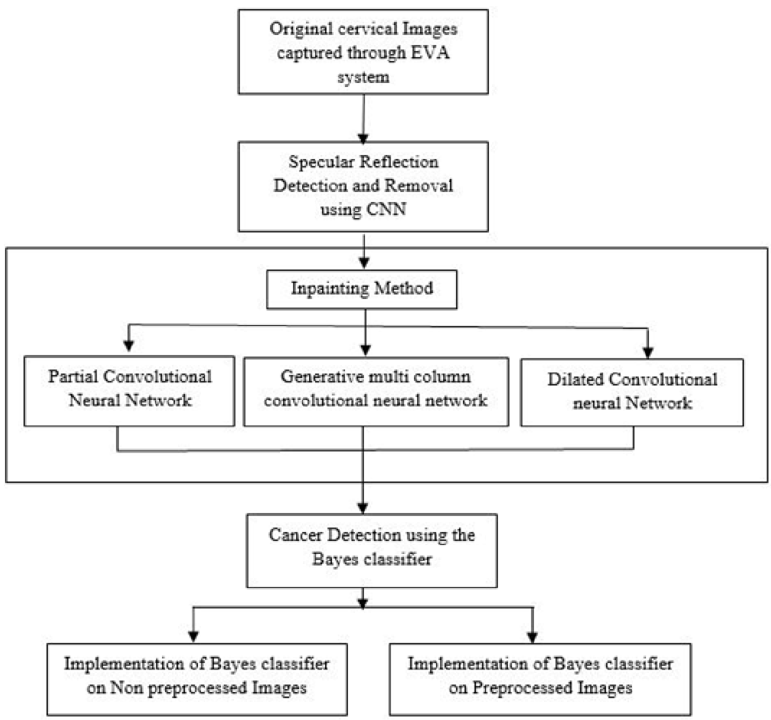

3.1 Specular reflection detection and removal

Specular reflection appears as the noise during the analysis of the acetowhite region because these glare regions appear similar to the acetowhite regions. The specular reflection has the properties of low saturation and high-intensity pixel values. The pixel with the high-intensity values is taken as the feature values for the detection of specular reflection on the cervical images. The intensity value of the digital image ranges from 0–255, where 0 represents the black and 255 represents the white pixel value of the images. Based on the analysis, the pixels value ranges from 0–190 is taken as the non-specular region, and pixel value ranges from 191–255 is set as zero to represent the specular reflection regions. The extracted features are trained using a convolution neural network. The convolutional neural network for the detection and removal of glare region is constructed using one input layer, three hidden layers, and two output layers. It is built with the activation function of relu and sigmoid with the kernel size of 3*3 for the detection and removal of specular reflection region on the cervical images. The result obtained using the CNN specular are shown in the Figure 3.

Figure 3 The detected specular reflection on the cervical images. (a) the original images with the specular reflection. the black dotted box represents the region with the specular reflection. (b) the detected specular reflection which is highlighted with the yellow box (see online version for colours)

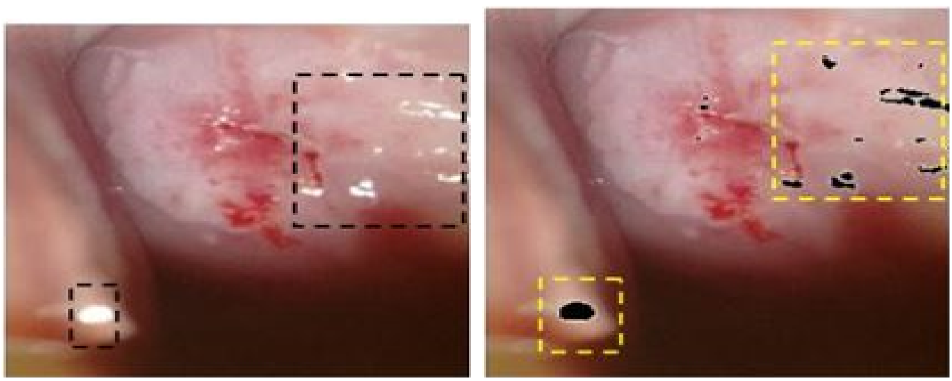

(a) (b)

Note: the black region on the image (b) represents the detected specular reflection.

This method helps in detecting the specular reflection region with high and low-intensity values. It is an important algorithm because some of the acetowhite regions are detected as the specular reflection will lead to the wrong refilling process. This algorithm accurately identifies the specular reflection without disturbing the acetowhite regions. The next section discusses, filling up the removed region of cervical cancer with the neighbouring pixels to improve the quality of the cervical images.

3.2 Inpainting method

The previous section discussed the detection and removal of specular reflection pixels on the cervical images. To fill the empty region of the cervix images, a deep learning inpainting algorithm is used in this methodology. The deep learning inpainting methods like P.Conv, generative multi-column convolution neural network (GMCNN), and D.Conv algorithm are used for filling the empty pixels on the cervical images captured through smart colposcopy. It helps to fill the empty regions and improve the quality of the cervical images for further analysis.

3.2.1 Inpainting using partial convolutional neural network (P.Conv)

Guilin et al. (2018) proposed a P.Conv for inpainting the digital images. It uses the stacked partial convolutional operation and updated binary mask to fill the missing pixels on the cervical images. For training the network, U-net architecture is used by replacing the encoder-decoder with the P.Conv. The following steps involved in the P.Conv are, partial convolutional operation, updating the binary mask and Network architecture.

3.2.1.1 Step 1 partial convolution operation

Partial convolution is expressed in the equation (1)

$$x' = \begin{cases} W^T (X \odot M) \dfrac{sum(1)}{sum(M)} + b, & if\ sum(M) > 0 \\ 0, & otherwise \end{cases} \quad (1)$$

where *W* and *b* are the corresponding kernel weight and bias, *X* is the pixel value, i.e., the feature value of the current sliding window. The *M* represents the binary mask which indicates the feature value where 0 represents the removed reflection regions (masked) and 1 represents the non-specular pixels (unmasked) on the cervical images. The scaling factor sum (1)/sum (*M*) uses the scaling to adjust the valid input pixels of the images.

3.2.1.2 Step 2 Updating of the binary mask

After the partial convolution operation, to update the mask region of the cervical images, the following condition should satisfy as in equation (2). If the convolution operation output has at least one valid input pixel, then it is marked as the valid pixels for the next partial convolution operation. This process is carried out until all the masked region becomes valid pixels. After updating the binary mask the U-net architecture is used to train the cervical images and fill the missing pixels.

$$m' = \begin{cases} 1, if\ sum(M) > 0 \\ 0, \quad otherwise \end{cases} \quad (2)$$

3.2.1.3 Step 3 Network architecture

The U-Net architecture is the convolutional neural network architecture highly used in biomedical images. The U Net architecture is built with the encoder-decoder along with the convolutional neural network (Isola et al., 2017). In this algorithm, the U-Net convolution layer is replaced with the partial convolution layer along with the skip links. It consists of the nearest neighbour up sampling in the decoding stage along with the skip links. The skip links connect two feature maps and two masks and act as a feature for the next partial convolution layer. The final layer of the partial convolution layer combines the cervical input image with a hole and is masked to fill up the empty region on the cervical images. The empty pixel refilled using the partial convolutional layer is shown in Figure 4.

3.2.2 Inpainting using generative multi-column convolutional neural network (GMCNN)

Wang et al. (2018) proposed the multi-branch convolutional neural network along with the dilated convolution neural network to refill the invalid region on the digital images. It is used with the cervical images captured through a smart colposcope to improve the quality of the images. For this multiple receptive filed method, the following steps are followed:

Figure 4 The specular reflection inpainting using a partial convolutional neural network. (a) the original images with specular reflection which is represented using the black box (b) the detected specular reflection using the cnn method which is represented using the red box (c) the partial convolutional inpainting method which is represented using the violet box (see online version for colours)

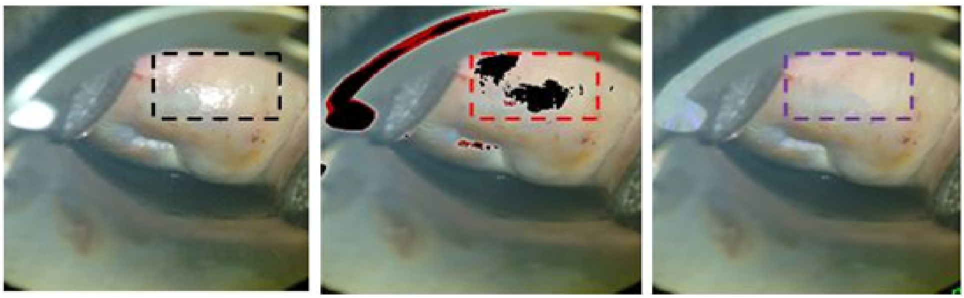

(a) (b) (c)

3.2.2.1 Step 1: The input and masked images

The input cervical images with the removed specular reflection region are considered as X and a binary mask *M* as input. The unknown pixels of the empty region of the cervical image *X* are filled with zero. After creating the input and masked images, the images are refilled using the network architecture called generative network.

3.2.2.2 Step 2: Network architecture

The generative network consists of three (n = 3) parallel encoder and decoder sections to extract the features from the input images X. Each receptive field uses three different kernel sizes like 3 × 3, 5 × 5, and 7 × 7 with the dilation rate of 1, 2, and 3, respectively. The three different kernel sizes used in three different branches are used for extracting features at different resolutions of the cervix images. The up-sampled is used at layer n = 1, 2 to increase the original resolution of the output cervical images. The output features F of the three branches are concatenated to the next two convolutional layers denoted as d (.) to produce the output image Y. The completed image (Y) is represented as Y = d (F). The generative networks are merged at one point and taken to the convolutional network to fix the missing pixels. The removed cervical region is refilled using the GMCNN method as shown in Figure 5.

The specular reflection was removed to create random holes in the cervical images. Some of the cervical regions are small holes, and some regions are large holes. The refilling process is successful for the region with small holes, and it does not affect the colour or the resolution of the cervical images. The large holes are also refilled, but the refilled large holes appeared as the small patches on the cervical images. So, it will affect the quality of lesion detection leading to the wrong analysis on the cervical images.

Figure 5 The specular reflection inpainting using generative multi-column convolutional neural network. (a) specular reflection represented using the black box (b) the red box represents the detected reflection region using CNN (c) the inpainted images using GMCNN represented using the violet box (see online version for colours)

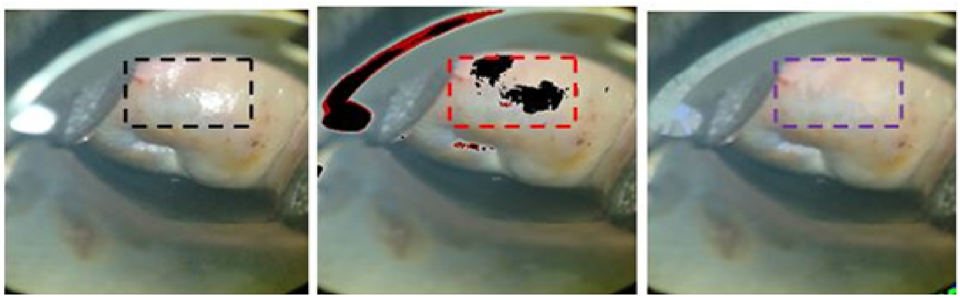

(a) (c) (b)

3.2.3 *Inpainting using dilated convolutional neural network (D.Conv)*

Salem et al. (2019) proposed the D.Conv for the randomly shaped missing region on the cervical images. The input and masked images are extracted and trained using the generator neural network to refill the removed reflection pixels with their neighbouring pixels.

3.2.3.1 Step 1 Input and masked images

The original cervix images captured through the EVA system are taken as the input images, and the detected specular reflection is converted to the binary mask to consider the missing region of the original images. The original cervical images and the binary masked images are taken as the input pair (corrupted images) for the generator to refill the missing pixels on the cervical images.

3.2.3.2 Step 2 Network architecture

To fill up the empty region of the cervical images, the generator inpainting (GI) network is used in this algorithm. The GI network is a fully convolutional neural network with the input of corrupted cervical images. The GI network is employed with the encoder-decoder architecture to reduce memory usage and computational time. The resolution of the resulted images gets affected as it undergoes the refilling operation on the empty region. But the resolution of the cervical images is more important for the analysis of dysplasia. The resolution of the cervix images is retained using the dilated convolutional neural. The dilated convolution operation is the modified version of the convolution operation which gives fast training with the minimum number of parameters. The training images are set to the size of 256x256 with the activation function of rectified linear unit (ReLU) and leaky ReLu with $\alpha = 0.2$ in the encoder region and decoder region respectively. The removed specular reflection on the cervical images is refilled using the D.Convs as shown in Figure 6.

The result obtained using the D. Conv algorithm helps in refilling the holes on the cervical images. The drawback is that the colour of some cervix images is affected and appears as some blue region on the images. The colour of the cervix images is more important for the neoplasm detection. In the refilling process, the small holes of the cervical images are filled, but the large holes refilled regions appear as the patches on the cervical images.

Figure 6 The specular reflection inpainting using dilated convolutional neural network (a) the original cervix images with the black box representing the specular reflection (b) the red box represents the detected specular reflection (c) the refilled pixel using dilated convolutional neural network (see online version for colours)

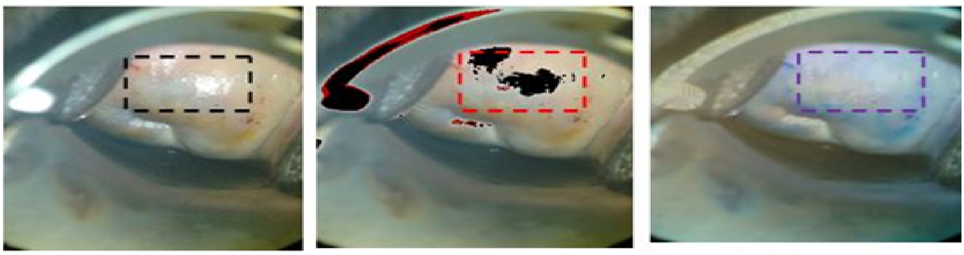

(a) (bc) (c)

3.3 Cancer detection using Bayes classification

Hariharan et al. (2012) used the Bayes classifer for the identification of dysplasia region on the cervical images. The dysplasia regions appear as the acetowhite region which will differ completely from the other cervical region. The acetowhite regions are manually marked as abnormal tissue of the cervical images to extract the features. To detect these lesion regions, initially statistical features are extracted from the normal and the lesion region of the cervical images. The extracted features are given to the Bayes classifier to detect the neoplasm on the cervical images which is captured through the smart colposcopy. The cervical images captured via the Eva system are split into the overlapping size of 32*32. For the detection of lesion region, the following methods are:

- Step 1: The RGB cervical images are divided into red, green and blue channels.
- Step 2: The statistical features are extracted from each channel for lesion recognition on cervical images. The statistical features like mean (μ), standard deviation (σ), and the skewness value are extracted from each colour channel of the cervical images.
- Step 3: The extracted statistical feature values are merged to identify the acetowhite region on the cervical images.
- Step 4: The feature extracted from each image is included in the analysis and adopted to train in the naïve Bayes classifier to identify the lesion region on the cervical images.
- Step 5: For the classification, the cervical images are trained with the 1,000 images which are downloaded from the Kaggle dataset. Type 2 (CIN2) and type 3 (CIN3) cervical images are considered for this algorithm, because type 2 and type 3 have the higher portion of the acetowhite region on the cervical images.

The two input images are used for the analysis of the cervical images for lesion detection. They are the non-enhanced cervical images and the enhanced cervical images. The non-enhanced cervical images are the raw data directly downloaded from the dataset with the specular reflection. The enhanced cervical images are the specular reflection inpainted images.

Figure 7 Cervical cancer detection on non-enhanced cervical images (a) represent the original image with the marked cancer region and reflection region (b) cancer detection on the non-enhanced images (see online version for colours)

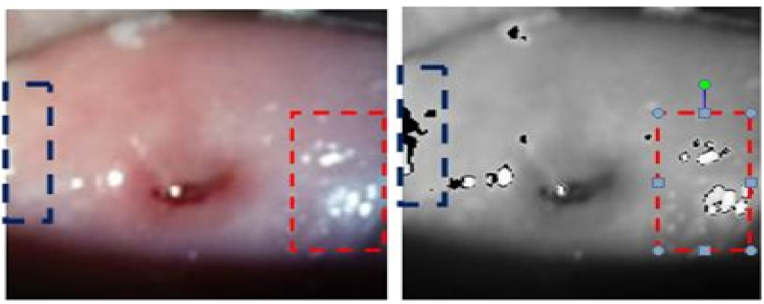

(a) (b)

3.3.1 Implementation of Bayes classifier non-enhanced images

The Bayes classifier algorithm is implemented on the non-enhanced images for cervical cancer detection. Figure 7(a) which represent the original image with high-intensity specular reflection is selected for this analysis. On analysing the non-enhanced cervical images, the Bayes classifiers detect the lesion region on the cervical images. Along with the lesion region, the specular reflection regions are also detected as lesion region on the cervical images as in the Figure 7(b). The red box represents the specular reflection region which is detected as a lesion region on the cervix images. The blue box represents the detected cancer region.

3.3.2 Implementation of Bayes classifier on the enhanced images

The Bayes classifier algorithm is implemented on the enhanced cervical images. The Figure 8(a) represents the original images in which the lesion region is marked and analysed with the physician for the correct prediction of cervical cancer. The cancer detection is applied to the enhanced cervical images using the deep learning refilling algorithm. The lesion detected on the partial convoluted inpainted cervical images gives the accurate prediction of cancer similar to the image marked on the original cervical images as shown in Figure 8(b).

Based on analysing the cervix images inpainted using the GMCNN algorithm, some white patches appear on the cervical images after applying the refilling algorithm. Along with the lesion identification these white patches region obtained are also detected as the lesion region on the cervical images leading to the wrong analysis of the cervical cancer as shown in the Figure 8(c). Similarly, the enhanced cervical images using the D.Conv refill the empty region with the patches on the cervical images. The colour of the images is also affected causing very difficult to analyse whether the lesion is correctly predicted or not as shown in Figure 8 (d). It shows that the quality of inpainting is more important because it will lead to wrong detection of the cancer region on the cervical images. For the quantitative evaluation, Cancer detected images are evaluated with the physician. Based on their suggestion, the result obtained using P.Conv inpainted images gives the accurate detection of dysplasia on the cervical images.

Figure 8 Cervical cancer detection on enhanced images (a) represent the original image with the marked cancer region. (b) the P.conv inpainting on the cervix images for lesion detection. (c) the GMCNN inpainting on the cervix images for lesion detection (d) the D.Conv inpainting on the cervix images for lesion detection (see online version for colours)

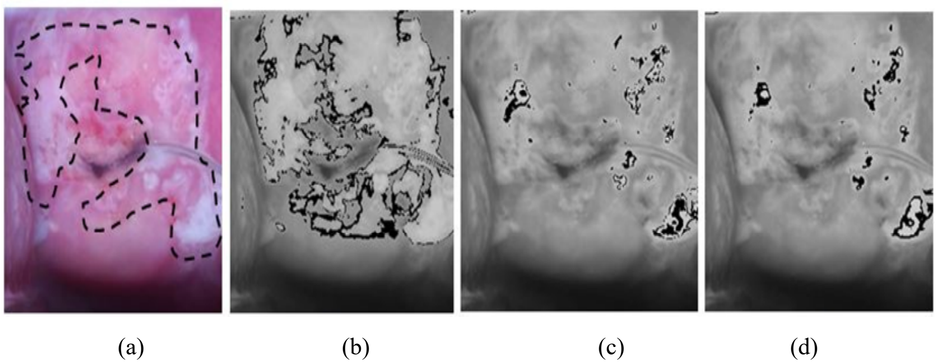

4 Experimental results

For the experimental setup, the smart colposcopy cervical images are downloaded from the Kaggle dataset (Kaggle, 2020). The Kaggle dataset provided more than 1,000 images in each folder of CIN1, CIN2, and CIN3 which are classified based on their grades of cancers. For the above algorithm, 500 images from CIN3, 250 from CIN2, and 250 images from the CIN 1 are selected from the dataset. The 1,000 images selected are resized to the size of 256*256. The algorithm explained is implemented using the Google Colab with the GPU processor of CUDA version 11.2. The quantitative analysis of the algorithm is explained in the next sections.

4.1 Specular reflection detection and removal on the cervical images

For the qualitative analysis, the accuracy, specificity, sensitivity, and precision are calculated for the detection of specular reflection on the cervical images. The accuracy determines the number of correctly identified reflection regions on cervical images divided by the total number of predictions on the cervical images. Precision is calculated as the ratio between the number of correctly identified specular reflections and the total number of glare regions on the smart colposcopy images.

Sensitivity is used to measure the ratio of correct specular reflection to the total number of specular reflection pixels from the cervical images. The specificity is the opposite of the sensitivity to calculate the ratio of region pixels that does not belong to total non-specular reflection to that which does not belong to the specular reflection regions. The CNN method gives accurate detection on the small and high-intensity specular regions with an accuracy of 98.03%. The qualitative analysis of the specular reflection is shown in Table 2.

Table 2 Qualitative analysis for the specular reflection detection

Methods	*Accuracy (%)*	*Specificity (%)*	*Sensitivity (%)*	*Precision (%)*
Specular reflection detection and removal using CNN	98.03	97.12	95.06	97.08

4.2 Inpainting method on cervical images

To evaluate the inpainting process, a qualitative metric like peak signal to noise ratio (PSNR) (Yuan et al., 2011), structural similarity index (SSIM), and Loss calculation (L1 and L2) (Liu et al., 2018) are used to calculate the quality of the predicted cervical images. The higher the PSNR value the higher the quality of the cervical images, and minimum the value of SSIM higher is the similarity of the predicted pixels on the cervical images. The value ranges of SSIM should be in the range of 0 to 1. The L1 and L2 are two loss functions that are highly used for minimising errors. The L1 loss function represents the LAB which is abbreviated as Least absolute deviations. The L1 loss function is the sum of the absolute difference between the original and predicted cervical images. The L2 loss function is calculated as the sum of all squared differences between the original images and the predicted cervix images. Minimum the loss percentage, the higher the quality of the cervical images.

Table 3 Comparison of the three deep learning inpainting algorithms for refilling the missing cervical images

	PSNR (db)	*SSIM*	*L1 Loss (%)*	*L2 Loss (%)*
P.Conv	48.25	0.984	0.627	0.286
GMCNN	47.32	0.981	0.632	1,204
D.Conv	47.48	0.807	0.851	0.811

The metrics mentioned above are used for calculating the qualitative of the predicted cervical images for the partial convolutional inpainting neural network, generative multicolumn convolutional neural network, and dilated convolution neural network. Based on the comparison of the above three methods, the partial convolutional network gives the higher quality for refilling the missing pixels on the cervical images. The comparison of the above three methods is shown in Table 3. The image result obtained using the inpainting algorithm is given in Table 4.

Table 4 The comparison of inpainting method using the P.conv, GMCNN, and D.Conv (see online version for colours)

Original images	*Specular reflection detection*	*Specular reflection removal*		
		P.Conv	*GMCNN*	*D.Conv*
	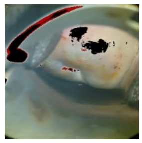	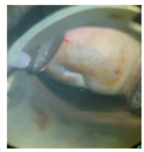		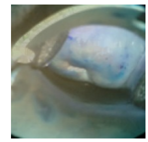
	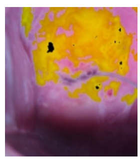	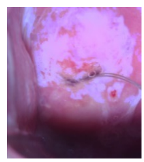	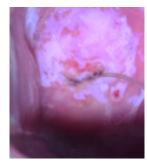	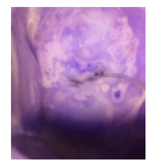
	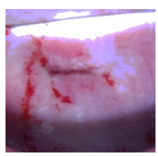	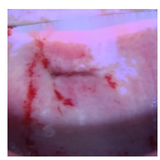	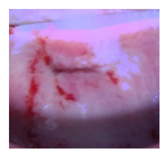	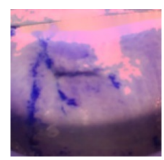
				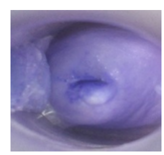
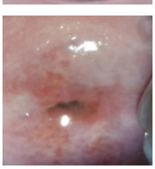		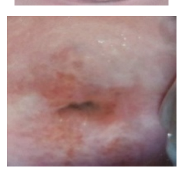	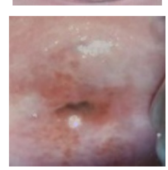	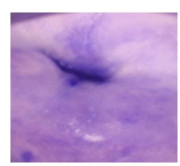
				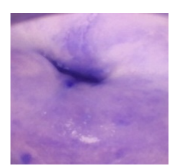
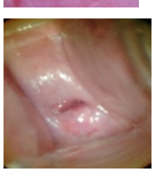	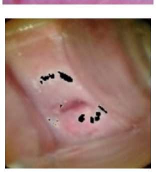	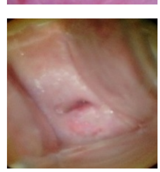	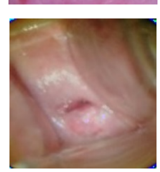	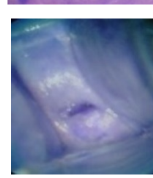
	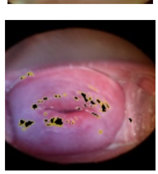	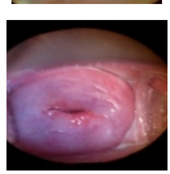	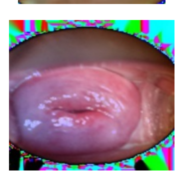	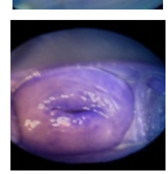

4.3 Dysplasia detection using Bayes classifier

The detection of the cancer region on the cervical images is calculated with accuracy, specificity, and sensitivity for the qualitative analysis. It is applied to the enhanced and the non-enhanced cervical images. Based on the analysis, the enhanced cervical images give higher quality of neoplasm detection on the cervical images. This shows that the quality of the cervical images is more important for the identification of the lesion region on the cervical images. On the comparative analysis of the three inpainting method, the enhanced images using P.conv algorithm give the accurate detection of cancer on the cervical images with an accuracy of 0.98% as shown in Table 5. The image result is of the cancer detection is shown in Table 6.

Table 5 Comparison of the three modified versions of convolutional neural network image for the cancer detection

	Specificity (%)	*Sensitivity (%)*	*Accuracy (%)*
P.Conv	0.90	0.92	0.98
GMCNN	0.82	0.90	0.92
D.Conv	0.86	0.92	0.96
Non Inpainted	0.63	0.61	0.64

5 Discussion

1. The CNN method is applied to detect the specular reflection which helps to identify the small and high-intensity reflection region on the cervical images. It is more important to identify the affected region to apply the refilling algorithm. If the detection is not correct, then the inpainting also will be a failure in cervical images.
2. The comparative analysis was done on the three deep learning inpainting methods. The methods like P.Conv, generative multicolumn convolutional neural network, and D.Conv. The metrics like PSNR, SSIM and loss calculation were considered for the calculation.
3. Based on quantitating and qualitative analysis, the P.Conv gives a higher quality of inpainting result when compared to the other two methods as shown in Figure 9. The loss percentage of the pixel is lesser for the P.Conv when compared with the other two methods.
4. To justify that, the quality of the cervical images is important for the detection of neoplasm. The cervical cancer is predicted using the naïve Bayes classifier on the enhanced and the non-enhanced cervical images. On analysing the detection of cervical cancer, the enhanced cervical images give the higher accuracy of neoplasm detection on the cervical images. Comparing the partial convolutional neural gives a good accurate detection of neoplasm on the cervical images as in Figure 9. because the other method detects cervical cancer along with the patch mark created during the inpainting process.

5 The image result obtained are consulted with Dr. A. Saraswathy specialised in Medicine and Applied Nutrition at Avinashilingam University. She is also a member of the All India Medical Science Association and Nutrition Society of India.

Table 6 Comparison of the three modified versions of convolutional neural network for inpainting cervix images (see online version for colours)

Original images	*Cancer detection on cervix images*		
	P.conv images	*GMCNN images*	*D.Conv images*
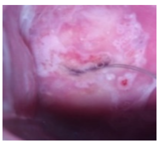	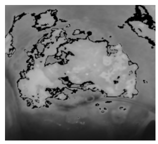	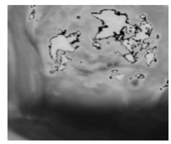	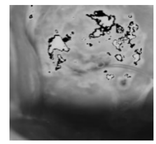
	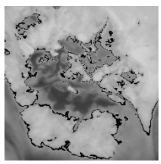	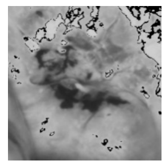	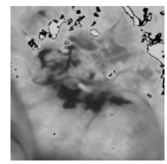
	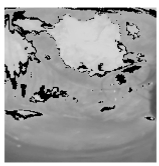	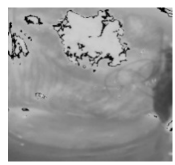	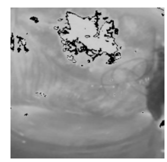
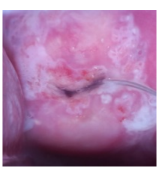	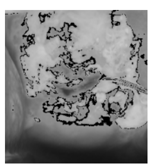	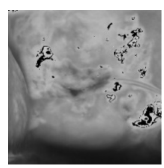	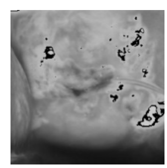
	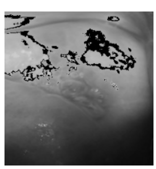	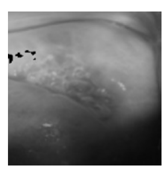	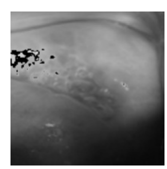
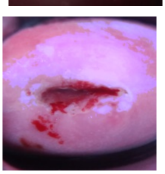		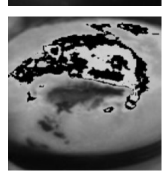	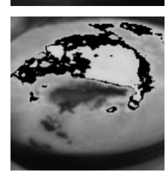

6 The suggestion from the expert is that cervical cancer is highly accurate in the partial convolutional layer neural network. Some non-cancer regions are also detected as the lesion region in the Bayes classifier algorithm. Based on her suggestion, the root regions of the cervical tissues are affected with cancer because of the slight colour change on the images which will grow as the pre-cancer stages in the future.

7 The cancer detection method is tried on the non-enhanced cervical images. The cancer region is detected, and all the specular reflection regions are also identified as cancer regions leading to wrong lesion detection.

8 The smart colposcope is introduced for the flexibility and time consumption screening procedure. The detection and removal of specular reflection takes only 10seconds, The partial convolutional inpainting algorithm improve the quality of the images in 40seconds and the neoplasm detection was carried out in 15 seconds.

Figure 9 Comparison analysis of the three deep learning inpainting methods on cervix images (a) the PSNR and SSIM value of the P.conv, GMCNN, and D.conv (b) the l1 and l2 percentage of the P.conv, GMCNN, and D.conv

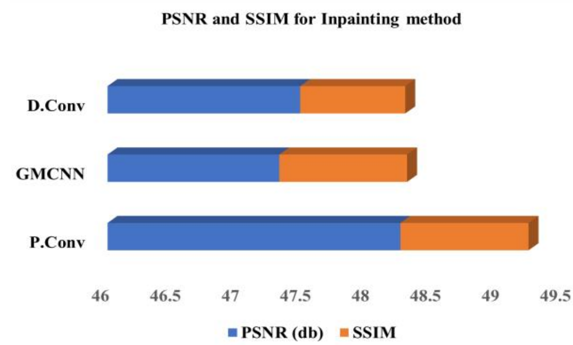

(a)

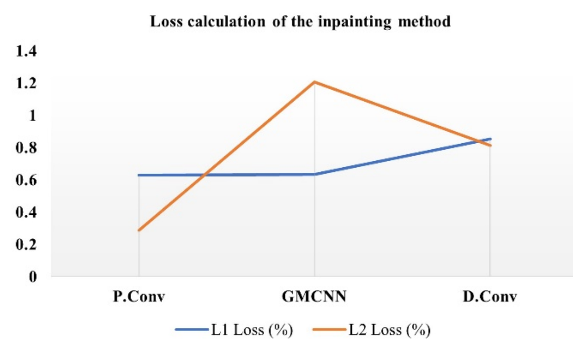

(b)

6 Conclusions

The smart colposcope is highly used for providing awareness and camps in various developing countries. But this specular reflection appears on the cervix images making it difficult for the analysis of the images. Here in this paper, the detection and removal of specular reflection are done on the cervix images. This method helps to identify the affected of noise on the cervical images. After the removal of the reflection region, the deep learning inpainting method is used to refill the void region on cervix images. The inpainting method consumes more time for training the algorithm. So, the deep learning inpainting method is training using the GPU with the CUDA version 11.2. Based on the comparative analysis the P.Conv gives the accurate prediction of the pixel value on the cervical images with less computation time of 40 seconds. The preprocessed images are used for dysplasia detection using the Bayes classifier algorithm. The algorithm is implemented on the non-preprocessed and preprocessed cervical images. On the analysis, the preprocessed cervical gives the accurate detection of cervical cancer on the cervix images. This algorithm helps to improve the smart colposcopy images and it will help to conduct screening camps with the minimum time and fewer experts.

Acknowledgements

The authors would like to express deep gratitude to the 'Centre for machine learning and intelligence' for supporting and sharing the resource for this research work. It is supported by the Department of Science and Technology under the scheme of DST CURIE (AI) sanctioned for the 'Core Research grant for Artificial Intelligence (AI)', in the year 2021–2023.

References

Arnold, M., Ghosh, A., Ameling, S. and Lacey, G. (2010) 'Automatic segmentation and inpainting of specular highlights for endoscopic imaging', *EURASIP Journal on Image and Video Processing*, Vol. 2010, No. 1, pp.1–12.

Balasubramaniam, G., Gaidhan, R.H., Khan, A., Saoba, S., Mahantshetty, U. and Maheshwari, A. (2021) 'Survival rate of cervical cancer from a study conducted in India', *Indian Journal of Medical Sciences*, Vol. 73. No. 2, pp.203–11.

Das, A., Kar, A. and Bhattacharyya, D. (2011) 'Elimination of specular reflection and identification of ROI: The first step in automated detection of cervical cancer using digital colposcopy', *2011 IEEE International Conference on Imaging Systems and Techniques*, Penang, pp.237–241.

Deepak, P., Philipp, K., Jeff, D., Trevor, D. and Alecei, A.E. (2016) 'Context encoders: feature learning by inpainting', *IEEE Conference on Computer Vision and Pattern Recognition* (CVPR) 2016, Las Vegas, Nevada, USA, pp.2536–2544.

Demir, U. and Unal, G.B. (2018) 'Patch-Based Image Inpainting with Generative Adversarial Networks' Computer vision and pattern recognition, [online] https://arxiv.org/abs/1803.07422 (accessed on 13 January 2022).

Goldbloom, A. and Ben, Hamner. (2010) *Kaggle* [online] https://www.kaggle.com/c/intel-mobileodt-cervical-cancer-screening (accessed on 13 January 2022)

Guilin, L.F.A., Reda, K.J., Shih, T.C. and Tao, B.C. (2018) 'Image inpainting for irregular holes using partial convolutions', *Computer Vision and Pattern Recognition* [online] https://arxiv.org/abs/1804.07723 (accessed on 13 January 2022).

Huang, W.H., Chen, R.L. and Zhang, J.M. (2005) 'Improvement and implementation of objective digital video quality measurement', *Journal of Beijing University of Posts and Telecommunications*, Vol. 4, No. 4, pp.87–90.

Iizuka, S., Simo-Serra, E. and Ishikawa, H. (2017) 'Globally and locally consistent image completion', *ACM Transactions on Graphics* (TOG), Vol. 36, No. 4, pp.1–14.

Jiahui, Y., Zhe, L., Jimei, Y. and Xiaohui, S. (2019) 'Free form images inpainting using gated convolutional', *Computer Vision and Pattern Recognition* [online] https://arxiv.org/abs/1806.03589 (accessed on 13 January 2022).

Kaggle [online] https://www.kaggle.com/(accessed on 13 January 2022)

Karapetyan, G. and Sarukhanyan, H. (2013) 'Automatic detection and concealment of specular reflections for endoscopic images', *Ninth International Conference on Computer Science and Information Technologies*, King Mongkut's University of Technology North, Yerevan, Armenia, pp.1–8.

Lange, H. (2005) 'Automatic glare removal in reflectance imagery of the uterine cervix', in *Medical Imaging 2005: Image Processing. International Society for Optics and Photonics*, San Diego, California, United States, pp.2183–2192.

Lee, N.C., Wong, F.L., Jamison, P.M., Jones, S.F., Galaska, L., Brady, K.T., Wethers, B. and Stokes T.G.A. (2014) 'Implementation of the national breast and cervical cancer early detection programme: the beginning', *Cancer*, Vol. 120, No. S16, pp.2540–2548.

MobileODT [online] https://www.mobileodt.com/(accessed on 13 January 2022)

Nermin, M.S., Hani, M., Mahdi, K. and Hazem, M.A. (2019) 'Random shaper images inpainting using dilated convolutional neural network', *International Journal of Engineering and Advanced Technology* (IJEAT), Vol. 8, No. 6, pp.641–647.

Pallavi, V. and Payal, K. (2011) 'Automated analysis of cervix images to grade the severity of cancer', *Annual International Conference of the IEEE Engineering in Medicine and Biology Society*, Massachusetts, USA, pp.3439–3442.

Pathak, D., Krahenbuhl, P., Donahue, J., Darrell, T. and Efros, A. (2016) 'Context encoders: feature learning by inpainting', *2016 IEEE Conference on Computer Vision and Pattern Recognition (CVPR)*, Las Vegas, USA, pp2536–2544.

Rahman, M.R.A., Emdadul, S., Golam, M., Sharmin, N.R. and Choudhury, S.A. (2013) 'Beating cervical cancer in the developed countries: a dream or a reality' public health [online] https://www.intechopen.com/chapters/44592 (accessed on 13 January 2022).

Reichheld, A., Mukherjee, P.K., Rahman, S.M., David, K.V. and Pricilla, RA. (2020) 'Prevalence of cervical cancer screening and awareness among women in an urban community in South India–a cross sectional study', *Annals of Global Health*, Vol. 86, No. 1, pp.1–7.

Wang, X., Li, P., Liv, Y., Xue, H., Xu, T., Du, Y. and Liu, P. (2021) 'Integration of global and local features for specular reflection inpainting in colposcopic images', *Journal of Healthcare Engineering*, Vol. 2021, No. 1, pp.2411–2502.

Wang, X., Xiaojuan, Q., Xiaoyong, S. and Jiaya, J. (2018) 'Image inpainting via generative multi-column convolutional neural networks', *Computer Vision and Pattern Recognition*, [online] https://arxiv.org/abs/1803.07422 (accessed on 13 January 2022).

Xiaolei, H., Wei, W., Zhiyun, X. and Sameer K.A. (2008) 'Tissue classification using cluster features for lesion detection in the digital cervigram', *EURASIP Journal on Image and Video Processing*, Vol. 2010, No. 1, pp.1–12.

Yuan, F., Huang, L.F. and Yao, Y. (2011) 'Research on objective assessment methods of video quality', *Journal of Video Engineering*, Vol. 31, No. 9, pp.91–94.

Measurement: Sensors 27 (2023) 100788

Contents lists available at ScienceDirect

Measurement: Sensors

journal homepage: www.sciencedirect.com/journal/measurement-sensors

Improvising grading of cervical cancer using quality assessment method in smart colposcopy images

M.B. Jennyfer Susan *, P. Subashini

Department of Computer Science, Centre for Machine Learning and Intelligence, Avinashilingam Institute for Home Science and Higher Education for Women, Coimbatore, India

ARTICLE INFO

Keywords:
Specular reflection
Smart colposcopy
Cervical cancer
Grading system
Binary masking

ABSTRACT

Smart Colposcopy is a low-cost and highly effective screening device used to detect cervical cancer. However, the captured images can be significantly affected by specular reflection, resulting in reduced accuracy during the grading process. In this paper, proposed a novel approach to enhance the accuracy of cervical cancer grading by addressing the issue of specular reflection. Here the method employs binary masking to identify the glare region and fine-tuned U-Net model to perform segmentation. Partial convolutional inpainting is used to replace the segmented region with neighboring pixels, effectively removing the glare from the images. The resulting enhanced images are then fed into classification models, including DenseNet121, Vgg19, and Efficient Net, which are trained to accurately grade cervical cancer. Experimental results demonstrate that our proposed method significantly improves the accuracy of cervical cancer grading, achieving accuracy rates of 97.32%, 96.25%, and 96.75%, respectively.

1. Introduction

Cervical cancer is a significant global health problem, especially in developing countries where access to advanced medical facilities and clinical resources is limited, resulting in high mortality rates. The World Health Organization (WHO) released statistics showing that cervical cancer is the fourth most common malignancy worldwide, with a reporting rate of 604 000 new cases and 342 000 deaths in the year 2020. In low- and middle-income nations, new cases and deaths accounted for around 90% of the global total in 2020 [1–3]. It is a condition where abnormal cells develop on the surface of the cervix which is caused by the Human Papilloma Virus (HPV). The severity of the condition is classified into three grades – mild (CIN1), moderate (CIN2), and severe (CIN3) - based on the extent of abnormal cell growth in the cervical tissues. CIN 1 refers to abnormal cells affecting the lower one-third of the epithelial layer, CIN 2 refers to abnormal cells affecting the lower two-thirds of the layer, and CIN 3 refers to abnormal cells affecting the full thickness of the epithelium. Screening is the primary preventive strategy for reducing mortality rates, but current screening methods, such as Pap testing, biopsy, and HPV testing, are invasive, expensive, and require advanced laboratory setup, making them highly inefficient in rural and tribal regions [4,5].

To overcome this challenges the smart colposcopy device is introduced to examine the cervical regions. In the recent year the detection rate of the diseases has increased using the images. Smart colposcopy images are a medical device that utilized IoT technology to provide enhanced visualization and diagnostic capabilities during colposcopy exams. The device transmit the patient data and imaging results to remote healthcare providers, improvising access to care and facilitating more timely diagnosis and treatments. The most advantage of the smart colposcopy device is the ability to capture high quality images of cervix, which can be analyzed and graded immediately. The screening programs have successfully reduced the incidence of cervical cancer by up to 80% in developing nations [6]. However, accurate grading of cervical dysplasia remains a challenge, with various deep learning classification models yielding low accuracy due to noise present in the images, such as specular reflection, which appears similar to acetowhite regions (dysplasia) on colposcopy images [7–9]. Specular Reflection occurs when light reflects off a shiny surface, such as the moist surface of the cervical tissue, creating a bright, glaring spot in the images as in Fig. 1. It can lead to misinterpretation of the images, particularly during the grading process, which can impact the accuracy of diagnosis and treatment. The specular reflection can obscure the color and texture of the cervical tissue making it difficult to differentiate between normal and

* Corresponding author.
E-mail addresses: 19phcsf008@avinuty.ac.in (M.B. Jennyfer Susan), subashini_cs@avinuty.ac.in (P. Subashini).

https://doi.org/10.1016/j.measen.2023.100788
Received 15 February 2023; Received in revised form 6 May 2023; Accepted 10 May 2023
Available online 30 May 2023

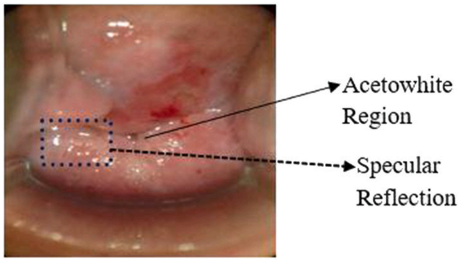

Fig. 1. Specular Reflection with acetowhite region on the cervical images captured through Eva system.

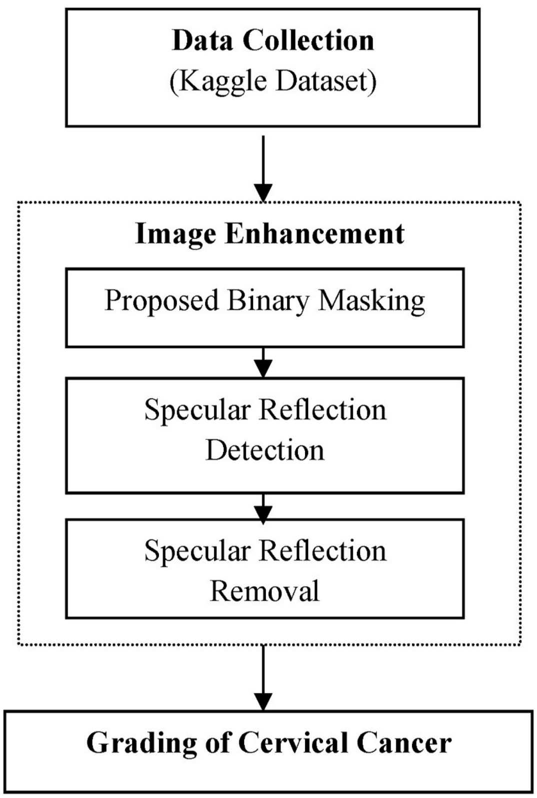

Fig. 2. Flow diagram of the methodology.

abnormal tissues. So it is necessary to remove the specular reflection from the smart colposcopy images.

In this paper, proposed a method for identifying of specular reflection using the proposed binary masking and trained the images using U-Net model for the segmentation of specular reflection on smart colposcopy images. The segmented region is filled with neighboring pixels using a partial convolutional neural network to remove glare noise. The enhanced and unenhanced smart colposcopy images to demonstrate the importance of removing specular reflection for accurate cervical cancer grading. The paper's contributions include a new approach for glare reduction, and experimental results show significant improvements in classification accuracy. This paper's structure includes related work on specular reflection detection and inpainting, methodology for enhancement and grading, experimental results and analysis, and conclusion.

2. Related works

Specular Reflection appears as the white intensity on the cervical images. It almost appears like the dysplasia region or acetowhite region and covers a certain region of the cervical images with its reflection properties. The detection of specular reflection is highly predicted by applying threshold on the color space model. Inpainting is the traditional method highly used in digital images for refilling the missing pixels. During earlier times, many detections and inpainting methods have been proposed for the removal of specular reflection removal but very little method is automated. During recent years the computer vision along with the deep learning algorithm are highly used for inpainting the missing pixels. Attard et al. [10] proposed the color based approach along with the deep learning model for the prediction of specular reflection on the object images. It uses the mean value of the RGB color pixel to predict the glare portion of the colposcopy images. The masked image is trained using the deep learning model to identify the affected portion. The model predicts the glare region with the frequency weight IOU with 0.83 and means IOU with 0.75. Das et al. [11] proposed the color space based morphological operation for the prediction of specular reflection on cervical images. The each plane of the RGB color space is extracted using AND operation to highlight the white region on the images. The morphological operation is applied to mark the outline of the reflection region. The reflection identified are which are marked are removed using the Laplace equation. The above method is used as the preprocessing method to identify the area of interest in the cervical images.

Anwar et al. [12] proposed SpecSeg for the prediction of specular highlight on the digital images which identifies the highlighted and label glare region. The labeled regions are trained using the U-Net model with the epoch value of 200. The specular highlights are predicted with the meanF1 value of 0.502 and MAE value of 0.008. The training time of the model is reduced to 40 min compared to the existing method. Pallavi et al. [13] used the histogram value is for the detection of glare region on the cervical images G component of the RGB color space is extracted from the images. The histogram is applied to remove the local minima region for the G component to extract the glare region. It is used as the preprocessing method to improvise the quality of the cervical cancer detection. Deepak et al. [14] used the GAN model with encoder decoder pipeline to predict the missing region of the images. The AlexNet with one stride convolutional and feature map is used along with the activation function to extract the feature from the neighboring pixels. The mean value is computed to predict the missing pixels on the digital images. The proposed method predicts the Mean L1 loss value of 9.37%, Mean L2 Loss value of 1.96% and PSNR value of 18.58 db. Lizuka et al. [15] proposed the dilation convolutional along with the local and global discriminator for the prediction of missing pixels. The neural dilation network increases the speed of the feature extraction on the digital images. The local and global context discriminator predicts the empty region and fills the region with the relevant pixels. The global context discriminator takes the complete input images and the local context discriminator completes the small empty portion of the input images. The proposed method fixes the low resolution output images compared to the context encoder method. It is used in many digital images to predict the missing region on the images.

Demir et al. [16] 2018 used the patch generative adversarial network for the prediction of damaged region on the digital images. The generated network uses the corrupted images to constructs the pixels. The ResNet is used along with the generative network to fill the large hole in the digital images. The proposed predict the missing pixel with the L1 loss of 5.42 and L2 loss of 1.16. The PSNR value and SSIM value of the predicted pixel is 18.9 and 0.884 respectively. Yu et al. [17] proposed the Gated Convolutional Neural Network is proposed for the identification of missing pixels. The model is built with the SN path and GAN model. The learnable version of the network validates the feature value which is activated with the sigmoid function. This method outperform in filling the random missing pixels. Chang et al. [18] used the convolutional Neural network to remove the glare region on digital images. The CNN model is end to end with the encoder and decoder and trained to remove directly the glare region on the digital images. The loss function

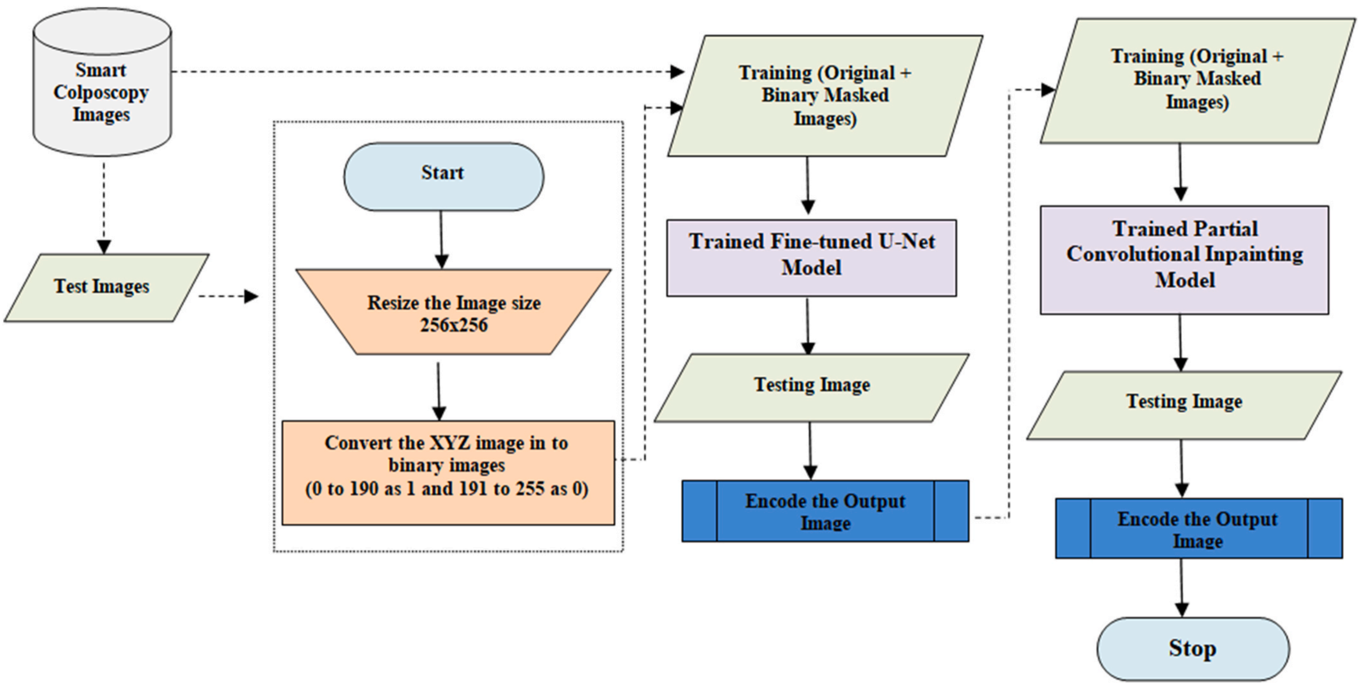

Fig. 3. Image enhancement on smart colposcopy images.

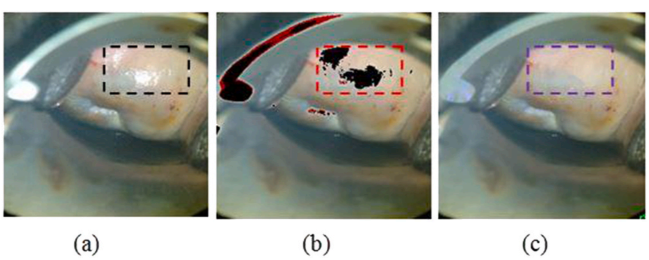

Fig. 4. Specular reflection inpainting using a partial convolutional neural network. (a) The original images with specular reflection which is represented using the black box (b) The detected specular reflection using the CNN method which is represented using the red box (c) The partial convolutional inpainting method which is represented using the violet box. (For interpretation of the references to color in this figure legend, the reader is referred to the Web version of this article.)

Table 1
Network architecture of the DenseNet 121.

Layer Name	Output Size	Filter Size/Stride
Input	255x255x3	–
Conv2D	127x127x64	7x7/2
MaxPooling2D	63x63x64	3x3/2
Dense Block 1	63x63x256	–
Transition Layer 1	31x31x128	1x1/1 + 2x2/2
Dense Block 2	31x31x512	–
Transition Layer 2	15x15x256	1x1/1 + 2x2/2
Dense Block 3	15x15x1024	–
Transition Layer 3	7 × 7 × 512	1x1/1 + 2x2/2
Dense Block 4	7 × 7 × 1024	–
Global Average Pooling	1 × 1 × 1024	–
Dense	1 × 1 × 3	–

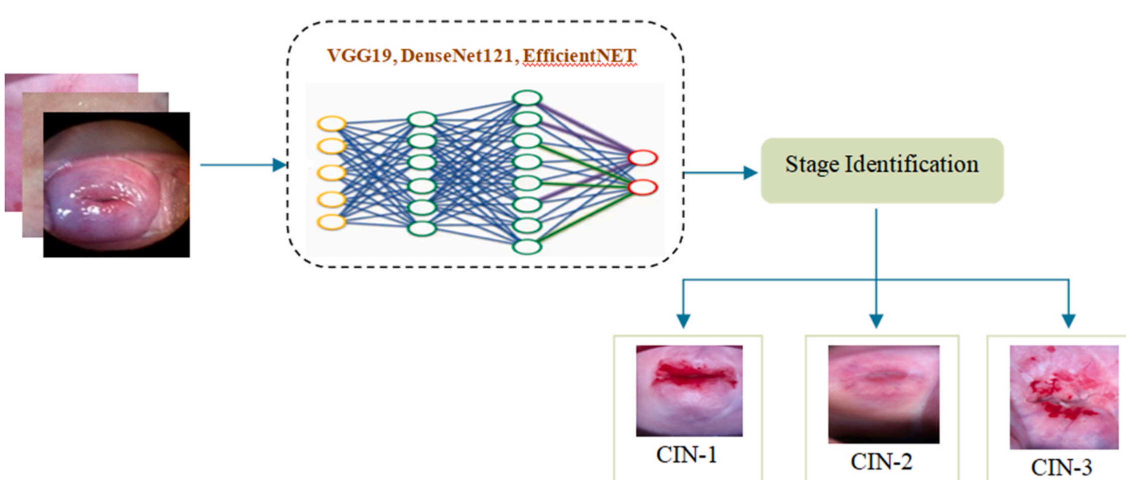

Fig. 5. Grading of cervical cancer using deep learning classification model.

Table 2
Network architecture of the Vgg19.

Layer Name	Output Size	Filter Size/Stride
Input	255x255x3	–
Conv2D	255x255x64	3x3/1 (same padding)
Conv2D	255x255x64	3x3/1 (same padding)
MaxPooling2D	127x127x64	2x2/2
Conv2D	127x127x128	3x3/1 (same padding)
Conv2D	127x127x128	3x3/1 (same padding)
MaxPooling2D	63x63x128	2x2/2
Conv2D	63x63x256	3x3/1 (same padding)
Conv2D	63x63x256	3x3/1 (same padding)
Conv2D	63x63x256	3x3/1 (same padding)
Conv2D	63x63x256	3x3/1 (same padding)
MaxPooling2D	31x31x256	2x2/2
Conv2D	31x31x512	3x3/1 (same padding)
Conv2D	31x31x512	3x3/1 (same padding)
Conv2D	31x31x512	3x3/1 (same padding)
Conv2D	31x31x512	3x3/1 (same padding)
MaxPooling2D	15x15x512	2x2/2
Conv2D	15x15x512	3x3/1 (same padding)
Conv2D	15x15x512	3x3/1 (same padding)
Conv2D	15x15x512	3x3/1 (same padding)
Stride Conv2D	15x15x512	3x3/1 (same padding)
MaxPooling2D	7 × 7 × 512	2x2/2
Flatten	25 088	–
Dense	4096	–
Dense	4096	–
Dense	3	–

Table 3
Network architecture of the efficient net.

Layer Name	Output Size	Filter Size/Stride
Input	255x255x3	–
Conv2D	255x255x64	3x3/2 (same padding)
Batch Normalization	128x128x32	–
Swish	128x128x32	–
MBConvBlock1	64x64x32	–
MBConvBlock2	64x64x16	1x1/1
MBConvBlock3	64x64x24	3x3/2
MBConvBlock4	32x32x24	–
MBConvBlock5	32x32x40	3x3/2
MBConvBlock6	16x16x40	–
MBConvBlock7	16x16x80	3x3/2
MBConvBlock8	8 × 8 × 80	–
MBConvBlock9	8 × 8 × 112	3x3/1
MBConvBlock10	8 × 8 × 192	5x5/2
MBConvBlock11	4 × 4 × 192	–
MBConvBlock12	4 × 4 × 320	3x3/1
Conv2D	4 × 4 × 1280	1x1/1
Batch Normalization	4 × 4 × 1280	–
Swish	4 × 4 × 1280	–
Global Average Pooling	1 × 1 × 1280	1x1/3
Conv2D		–

Table 4
Quantitative analysis for the detection of specular reflection on smart colposcopy images.

Methods	Binary Accuracy (%)	IoU	Dice-Coefficient	Loss value
Proposed Binary masking with Fine-tuned U-Net	0.989	0.965	0.981	−0.980
Proposed Binary masking with U-Net [15]	0.972	0.967	0.977	−0.984
Proposed Binary masking with Simple CNN [17]	0.924	0.915	0.921	1.269

is optimized to predict the pixel on the digital images Based on comparison analysis of the proposed method predict the glare region with the higher accuracy.

3. Proposed methodology

Kaggle dataset, which were affected by the noise called specular reflection. To improve the classification based on their stages (i.e., CIN1, CIN2, and CIN3), the collected cervical images were enhanced using a series of steps. First, proposed binary masking was applied to the images. This was followed by the identification of the glare region in the images. Finally, the glare region was removed from the smart colposcopy images to improve their quality. After the enhancement process, the images were graded using a classification model to predict the stage of cervical cancer. The workflow of the methodology is shown in Fig. 2. In summary, the methodology used in this study involved collecting and enhancing smart colposcopy images using a series of steps, and then grading the images using a classification model to predict the stage of cervical cancer.

3.1. Enhancement method on smart colposcopy image

Specular reflection appears as the white bright pixel covering certain region affecting the quality of the images. The quality of the image is highly considered during the cancer region analysis process. Due to this white pixel it resembles similar to the cancer region and lead to misinterpretation. To improve the quality of the smart colposcopy images the specular reflection region are identified using the proposed binary masking and trained using the Fine tuned U-Net model to segment the glare portion from the images. The removed region are refilled the region with its neighboring pixel using the partial convolution inpainting method. The workflow of the images enhancement process on the smart colposcopy images is shown in Fig. 3.

Step 1: Proposed Binary Masking

Specular reflection has the property of the white bright intensity value which appears on the surface of the smart colposcopy images. Due to high-intensity properties, the pixel intensity value is considered as the feature to predict the glare region on the cervical images. The pixel intensity value of the digital images ranges from 0 to 255, with 0 denoting the image's darkest pixel value and 255 denoting the whitest pixel value of the digital images. Since it is a digital device the color representation varies on each device. To avoid that, the colposcopy image collected from the dataset is initially converted to XYZ color space. Because the XYZ color space is device independent and does not affect the color representation of the images on each device. The smart colposcopy images used in the study were obtained from the Kaggle dataset and resized to a uniform dimension of 256x256 using the bicubic interpolation algorithm, which is known for preserving better pixel quality in medical images [19]. The resizing was performed during the masking process to ensure that all images were of the same size for use in deep learning models. It helps in reducing the computation time during the training process. Each intensity value is manually analyzed to predict the glare region. Based on analyzing the intensity value of each pixel the specular reflection pixel falls on the intensity value ranges from 191 to 255 whereas the non-specular region falls intensity region of 0–190. The specular region and nonspecular region are labeled using the binary masking. The specular reflection pixel is rescaled and set as 0, while the other region is set as 1 as shown in the Algorithm.1. The masked images extracted are trained using the fine-tuned U-Net model.

Algorithm 1:

Input: *Image Dataset represented as a 2D array "pixel" with size (img_height, img_width)*

```
For each x in range 0 to (img_height - 1)
  For each y in range 0 to (img_width - 1)
  Convert the RGB color values of pixel at position (y, x) to XYZ color space Set
  current_pixel_intensity = value of "pixel" at position (y, x) in the XYZ color space
  Set current_pixel = value of "pixel" at position (y, x)
  If current_pixel >= 190
   Set value of "pixel" at position (y, x) to 1
      Else if current_pixel <= 191
  Set value of "pixel" at position (y, x) to 0
End
```

Step 2: Fine tuned U-Net Model for Specular Reflection Detection

The challenges faced in medical images analysis is the lack of dataset. The U-Net model performance is higher for the segmentation process with minimum dataset especially for the medical images [20]. So in this paper, the U-Net model is fine tuned which is made suitable for the segmentation of the specular reflection on the colposcopy images. It is made up of an expanding path, which is used to decode the features of

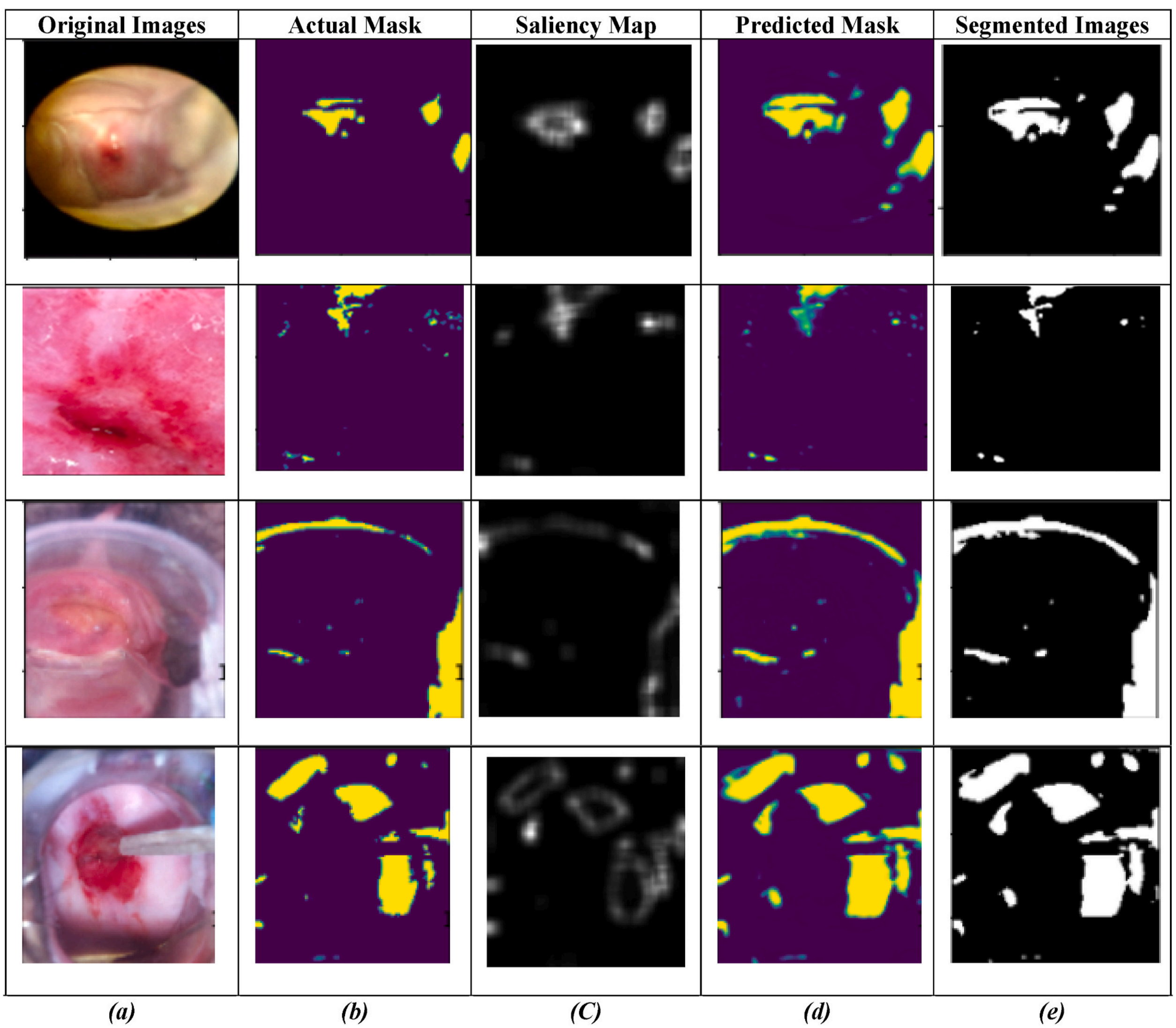

Fig. 6. Specular reflection region segmented using the proposed binary masking and Fine tuned U-Net model.

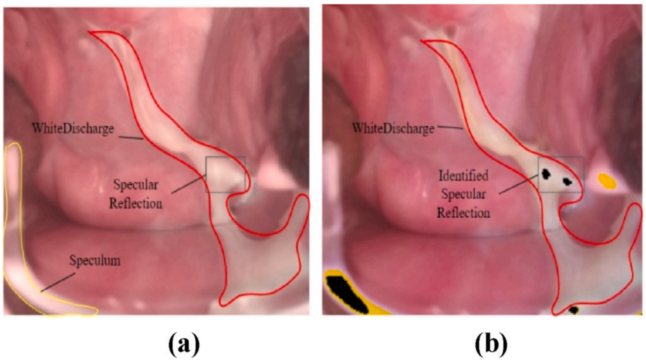

Fig. 7. Detection of speuclar reflaction without affecting the white portion on the digital images. (a) Represent the original images with the specular reflection and white discharges. (b) Represents the segmented specular reflection without affecting the white discharges.

Table 5
Quantitative analysis for the inpainting the smart colposcopy Images.

	PSNR (db)	SSIM	L1 Loss(%)	L2 Los(%)
P.Conv	48.25	0.984	0.627	0.286

the digital images, and the contraction path, also known as the encoder segment the feature regions. The model is built with four convolutional blocks where each block two convolution layers in both the encoder and decoder side of the model. The convolutional layer used in the U-Net model is represented in equation. 3.

$$F_{i,j} = f\left(\sum_{m=0}^{2}\sum_{m=0}^{2} W_{m,n} I_{x+m,y+n} + W_b\right) \tag{3}$$

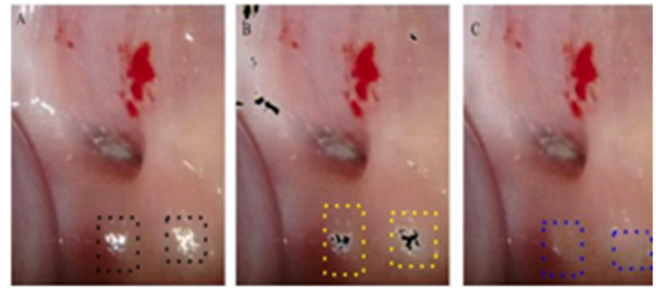

Fig. 9. Enhancement on Smart Colposcopy Images (a) Original Images (b) Specular Reflection Detection on smart Colposcopy Images (C) Removal of specular Reflection using Inpainting Method.

$W_{m,n}$ stands for the weight of the (m, n), $I_{x,y}$ stands for the row and column of the pictures, $F_{(i,j)}$ is the feature map generated from the smart colposcopy image. Each convolutional block consists of 3x3 convolutional layer followed by the rectified linear unit (ReLu) activation function. A 2x2 max pooling layer is follows each convolution block in the donwsampling and upsampling path.

The U-Net model is fine tuned for the improvising the detection of glare on the smart colposcopy images and its network architecture is represented in Algorithm.2. The batch normalization is enabled as true for each layer to speed up the convergence during model training. The dropout value is set as 0.2 for each layer of the down sampling region. The refined U-Net model has a neuron size or filter dimension of 8, 16, 32, 64, and 128 for the contraction path and 128, 64, 32, 16, 8 for the expansion path. The model is trained with the batch size of 10 and with the epoch value of 100. The model is boosted with the Adam optimizer with the learning rate of 0.00001. Since there are two classes (i.e. SR and Non-SR region) the binary cross entropy is used for the loss function. The input image size is set as 255x255x3, where the training dataset is set as (3870, 255, 255, 3) and testing dataset is set as (1000, 255, 255, 3).

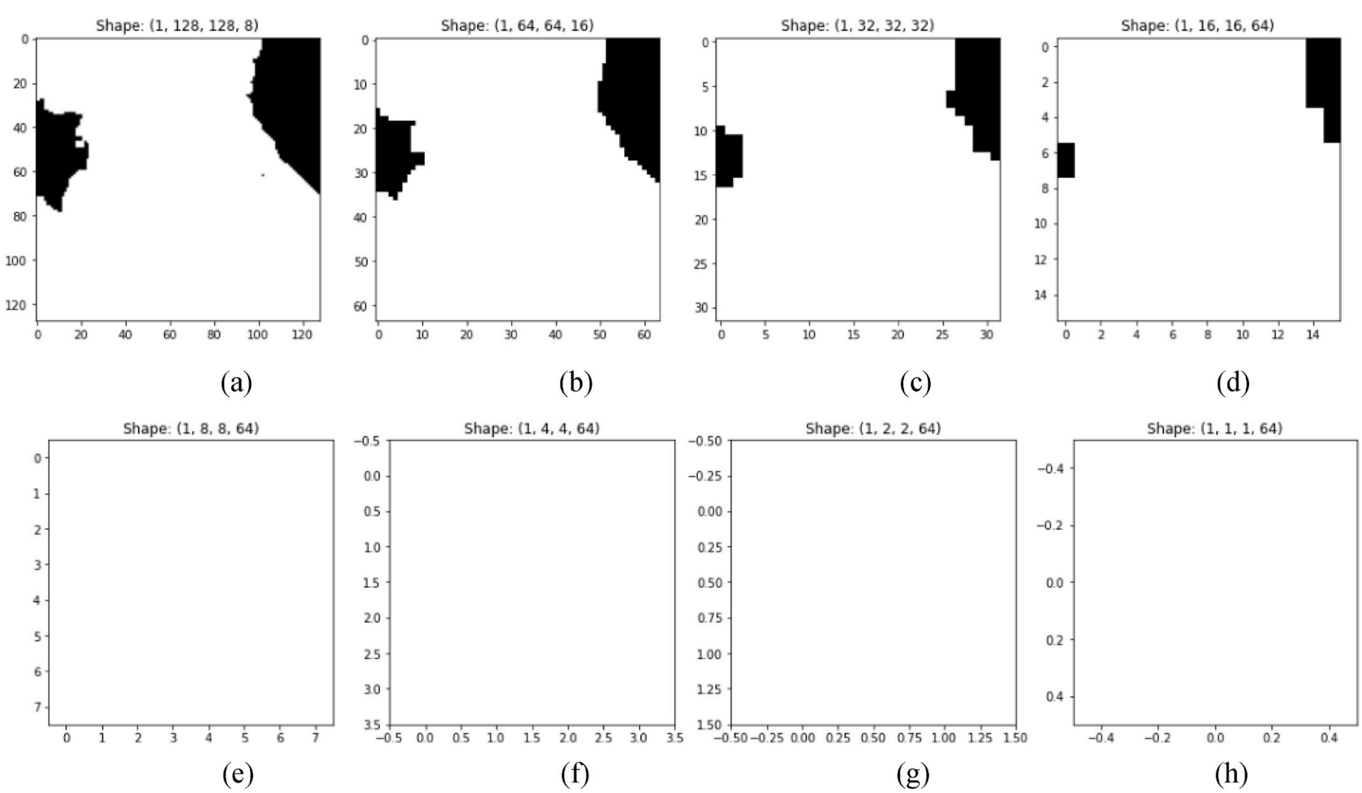

Fig. 8. Partial convolutional inpainting for filling the removed glare pixels.

Algorithm:2
Define *the U-Net model with input shape (255, 255, 3)*
Initialize *the model with 4 convolutional blocks*
For each *convolutional block:*
Add *a 3x3 convolutional layer with ReLu activation function*
Add *a 3x3 convolutional layer with ReLu activation function*
Add *a 2x2 max pooling layer*
Add *dropout with a value of 0.2*
Add *an expanding path to decode the features of the digital images*
For each *expanding block:*
Add *a 2x2 up-sampling layer*
Add *a 3x3 convolutional layer with ReLu activation function*
Add *a 3x3 convolutional layer with ReLu activation function*
Add *an output layer with sigmoid activation function*
Compile *the model with binary cross-entropy loss function and Adam optimizer with a learning rate of 0.00001*
Set *the batch size to 10 and the number of epochs to 100*
Set *the input image size to (255, 255, 3)*
Load *the training and testing datasets with sizes (3870, 255, 255, 3(Original and Masked Images)) and (1000, 255, 255, 3(Original and Masked Images)) respectively*
Train *the model on the training dataset*
Use the trained model to segment specular reflection on smart colposcopy images

The original and the masked images obtained from the proposed binary masking are taken as the input and trained the fine-tuned U-Net model for the segmentation of specular reflection from the smart colposcopy images. The masked image label the reflection region which need to be segmented and helps the.

Step 3: Removal of Specular Reflection on Smart Colposcopy Images

The specular reflections identified are removed using the partial convolutional inpainting method [21]. The partial convolutional neural network involves partial convolutional operation, updating binary mask and network architecture for filling the missing region on the smart colposcopy images. The partial convolutional is expressed in equation (4)

$$x^{'} = \begin{cases} W^{T}\ (I_{out} \odot M)\dfrac{Sum(1)}{Sum(M)}, if\ sum(M) > 0 \\ 0, Otherwise \end{cases} \tag{4}$$

Where X is the pixel value or the feature value of active sliding window, and W and b are the appropriate kernel weight and bias. The M represents the binary mask, which denotes the feature value. On the cervical images, the valid pixels are represented by 1 and the missing pixel by 0, respectively. The legitimate input pixels of the cervical images are

Table 6
Specular reflection detection and removal from the smart colposcopy images.

Original Images	Specular Reflection Detected Images	Removal of Specular reflection using Inpainted Images	Original Images	Specular Reflection Detected Images	Removal of Specular reflection using Inpainted Images
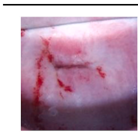		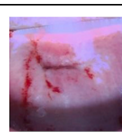	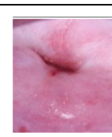		
	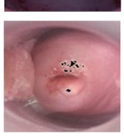	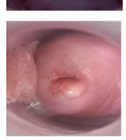			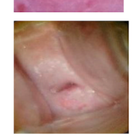
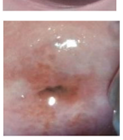	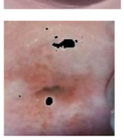	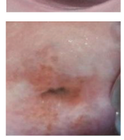		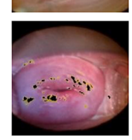	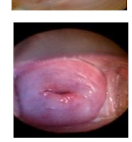

Table 7
Comparison of the classification metrics with enhancement and non enhancement images.

Metrics	Without Enhancement			With enhancement		
	DenseNet121	Vgg19	EffiecinNet	DenseNet121	Vgg19	EffiecinNet
Accuracy (%)	92.72	95.02	91.79	**97.32**	**96.25.**	**93.27**
Precision (%)	90.72	92.14	93.28	**96.89**	**95.74**	**95.74**
Specificity (%)	91.41	90.39	90.39	**94.73**	**91.39**	**91.39**
Sensitivity (%)	91.78	92.49	93.49	**92.12**	**90.79**	**90.79**

Table 8
The binary accuracy and Loss calculation for grading of cervical cancer at each epoch value.

<table>
<tr><th>With Out Enhancement</th><th>With Enhancement</th></tr>
<tr><td colspan="2">DenseNet121</td></tr>
<tr><td>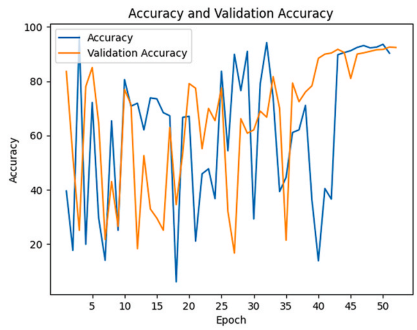
</td><td>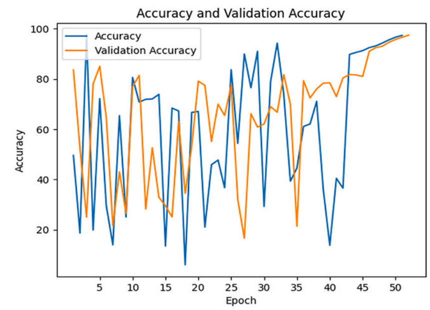
</td></tr>
<tr><td>
</td><td>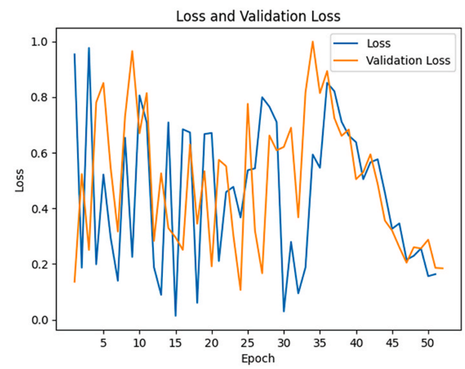
</td></tr>
<tr><td colspan="2">Vgg19</td></tr>
<tr><td>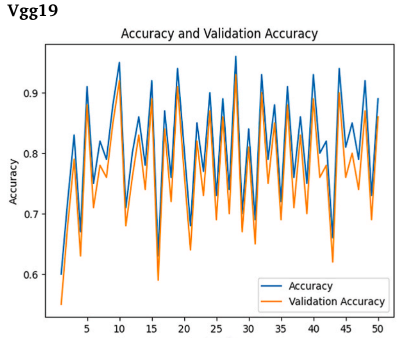
</td><td>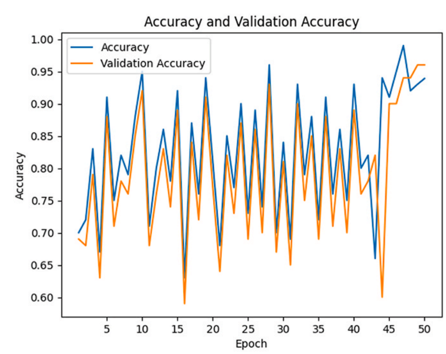
</td></tr>
<tr><td>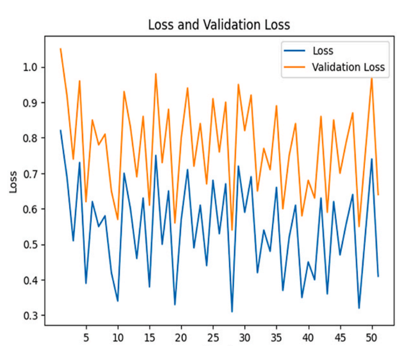
</td><td>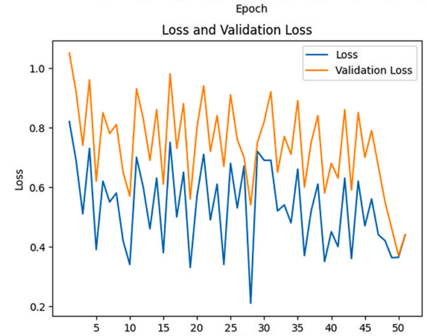
</td></tr>
<tr><td colspan="2">Efficient Net</td></tr>
</table>

(*continued on next page*)

Table 8 (*continued*)

With Out Enhancement	With Enhancement
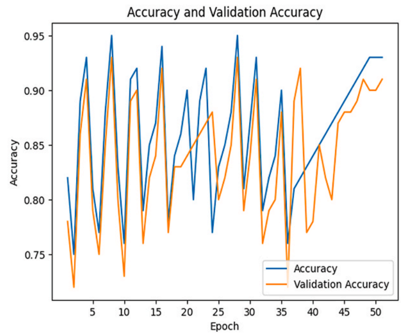	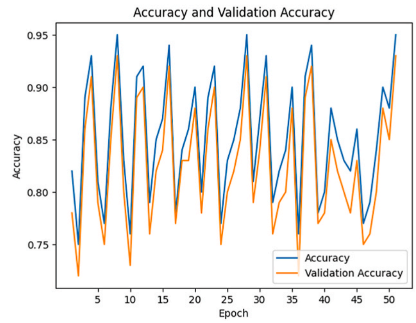
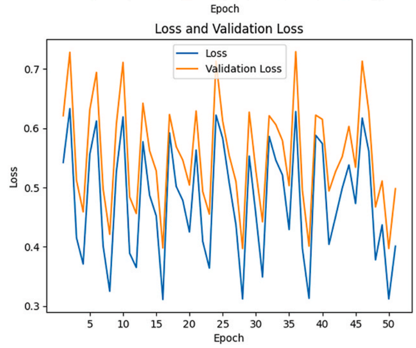	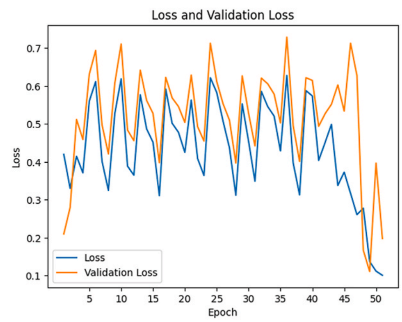

adjusted using the scaling by the scaling factor *sum (1)/sum (M)* as in the equation.5. The result of the convolution operation is designated as the valid pixels for the following partial convolution operation if it contains at least one valid input pixel. This procedure is repeated until all of the masking region's pixels are valid. The U-net model convolutional filter is replaced with the partial convolution filter for filling in the missing pixels in the colposcopy images when the binary mask has been updated.

$$m' = \begin{cases} 1, \mathit{if}\ sum(M) > 0 \\ 0, \mathit{otherwise} \end{cases}$$

For training the partial convolutional inpainting model the batch size is set as 32 with the epochs value as 100. The Adam Optimizer is set as 0.0001 with the L1 loss error and the learning rate is set as le^{-4}. The input image size if set as 255x255x3, where the training dataset is set as (3870, 255, 255, 3) and testing dataset is set as (1000, 255, 255, 3). The original and the masked images taken as the input and trained use the fine-tuned U-Net model for the prediction of specular reflection on the smart colposcopy images. The cervical input image is combined with a hole in the final layer of the partial convolution layer, which is then masked to fill in the hole. Fig. 4 depicts the empty pixel that was filled using the partial convolutional layer.

3.2. Grading of smart colposcopy images using classification models

The Cervical intraepithelial Neoplasia(CIN) are staged as CIN1, CIN2, and CIN3 based on the amount of the acetowhite region affected on the smart colposcopy images.

3.2.1. Network architecture

To classify the cervical cancer based on their types the classification model like DenseNet121, Vgg19, EfficientNet model are used in this paper as shown in Fig. 5 the model performance is calculated on the enhanced images and the unenhanced colposcopy images.

a. DenseNet121

DenseNet121 is the convolutional neural network used for the classification of the images. It was proposed by Hasan et al. [22] in the year 2017. The architecture of this model is based on the idea of densely connected layers. The DensNet takes the each layer as input and the feature maps of all proceeding layers. The architecture is built with 121 layers which is divided in to three blocks i.e., convolutional block, the transition block and the classification block, The convolutional block is build with the series of dense block, where each block consists of multiple of convolutional layer, batch normalization to reduce over fitting and ReLu activation function. The transition block consist of convolutional layer, a batch normalization layer and 1x1 global averaging pooling which reduce the spatial dimensionality of the feature maps to preserve the number of channels. The classification block is build with the global average pooling layer, a fully connected layer and softmax activation function to produce the classification result. The network architecture of DenseNet121 model used for the grading of colposcopy images is shown in Table .1.

b. Vgg19

VGG19 is a deep convolutional neural network architecture that was proposed by Simonyan and Zisserman in 2014. To grade the colposcopy images, the VGG19 convolution neural network, which has 19 layers, uses 16 convolutional layers and 3 fully connected layers are used. The convolutional layer is built with the 64 neurons with the filter size of 3x3 and 2x2 size of max pooling. The fully connected layer is built with the neuron size of 4096 which is followed by a dropout layer. The softmax layer is used in the output layer of the each class [17,23]. The network architecture of Vgg19 model used for the grading of colposcopy images is shown in Table .2.

b. Efficient Net

Efficient Net is the convolutional neural network introduced by Tan and Le [24] in the year 2019. The model is constructed with the MBConvBlock or Mobile Inverted residual bottleneck block. It is designed to reduce the number of parameters to maintain the higher accuracy of grading process. The input layer of the model is set as 255x255x3. The 64 convolutional layers is used with the filter size of 3x3 and stride value of 2x2. The same padding size is set, which does not affect the size of the image output image. In this model the swish activation function is used which is the combination of the sigmoid and ReLu activation function. The 12 MBConvBlocks are used, where each block is the combination of convolutional layer, point wise convolutional layer and skip connection. The MBConvBlock is repeated multiple times in the Efficient Net model with the variation of filter, strides and input/output dimension to reach the desired results. The point wise convolution layer applied 1x1 convolution to the output of the pervious layer and it increase the dimensionality of the output by maintaining the minimum number of parameters. The convolutional layer with the filter size of 1x1 maps the output of the previous layer to 1280 dimension feature space. The network architecture of Efficient Net model used for the grading of colposcopy images is shown in Table .3.

3.2.2. Training the classification model

The dataset is collected from the Kaggle dataset [17], which has three stages of cancer with a total of 4870 images. The model is divided in the ratio of 80% for training and 20% for testing the model. The model developed is trained with the dataset (3870, 255, 255, 3) and tested with the images (1000, 255, 255, 3). For training the input size of the image is set as 255x255x3 and the output class is 3 i.e., CIN1, CIN2 and CIN3. The batch size of the model is set as 32 with the learning rate of 0.0001. The model is trained with 60 epochs and trained with the Adam optimizer. The drop out layer is set as 0.5 to reduce the over fitting of the model due to the minimum number of dataset. The loss value is taken as sparse categorical cross entropy with the activation function of the softmax function. The weight initialize for the classification of the model is He normal to increase the performance of the model.

4. Experimental result and analysis

For the experimental setup, the smart colposcopy images are collected from the Kaggle dataset [25]. The implementation is carried out on the Google Colab with the hardware accelerator of 12 GB NVIDIA Tesla K80. In this section, the result obtained is analyzed in the both quantitative and qualitative analysis.

4.1. Specular reflection detection

The binary accuracy, the intersection of union (IoU), the dice coefficient, and the binary cross entropy are calculated for the quantitative analysis [20]. The intersection of union (IoU) identifies the overlap between the predicted mask and the original masked images of the smart colposcopy images. The binary accuracy predicts the total number of correctly predicted reflection regions divided by the total number of predictions on the smart colposcopy images. The dice coefficient determines the overlap region between the original and anticipated images by dividing the total number of pixels [26]. The binary accuracy, Intersection of Union, dice coefficient calculated for the prediction of specular reflection on smart colposcopy images is given in Table .4. The proposed binary masked images are trained using the fine-tuned U-Net model, U-Net model and the simple CNN model. The model is trained with the epoch value of 100. Based on the comparison analysis the proposed binary masking along with the Fine tuned U-Net model predicts the specular reflection with the accuracy of 98.91%. The computation time to attain is this model is 6 h 29 min with the memory usage of 15.74 GB.

Based on the qualitative analysis, the specular reflection region segmented using the fine-tuned U-Net is given in Fig. 6. In Fig. 6 (a) represent the original images collected from the Kaggle dataset. The predicted mask represents the images predicted by the model is shown in Fig. 6(b) and the actual mask represents the mask generated by the proposed binary mask which is given as the input to train the model Fig. 6(d). The detection of glare region in the layers of each fine tuned U-Net model layer is represented as the saliency map as given in Fig. 6(c). Finally the segmented images is the removed the glare region on the smart colposcopy images as shown in the Figure. (e).

The challenges faced in the removal of specular reflection are white discharge which also appears as white on the captured smart colposcopy images. But the proposed binary masking with the fine-tuned U-Net predict only the specular reflection region without affecting the other white portion of the smart colposcopy images as shown in Fig. 7.

4.2. Removal of specular reflection on smart colposcopy images

To evaluate the inpainting process, qualitative metrics like peak signal to noise ratio (PSNR) [21], Structural similarity Index (SSIM), and Loss calculation (L1 and L2) [27] are used to calculate the quality of the predicted cervical images. The higher the PSNR value the higher the quality of the cervical images, and minimum the value of SSIM higher is the similarity of the predicted pixels on the cervical images. The value ranges of SSIM should be in the range of 0–1. The L1 and L2 are two loss functions that are highly used for minimizing errors. The L1 loss function represents the LAB which is abbreviated as least absolute deviations. The L1 loss function is the sum of the absolute difference between the original and predicted cervical images. The L2 loss function is calculated as the sum of all squared differences between the original images and the predicted cervix images. Minimum the loss percentage, higher the quality of the cervical images. The PSNR, SSIM, L1 Loss and L2 loss calculated for the removal of specular reflection is shown in Table 5.

The partial convolutional layer is fixed in the U-Net model for inpainting the missing pixel of the images. So the model is using the eight layers during the filling process. Each layer the missing region will be reduced as the missing pixel is filled with the adjacent pixels. Fig. 8 (a) represent the glare region segmented using Fine tuned U-Net. From Fig. 8 (b)–(d), the size of the masked region is reduced because of it filling process. This process at each layer until the missing pixel is filled on the smart colposcopy images. Fig. 8 (e)–(h) are empty and no masked region (black region) are shown in the figure. It shows the images are completed filled in the layer 4 i.e., figure (d).

The smart colposcopy images with the specular reflection are shown in Fig. 9(a). The specualr reflection detected using the proposed U Net is shown in Fig. 9 (b) And the removal of specular reflection using the partial convolutional neural network is shown in Fig. 9 (C). The specular reflection removal has improvised quality of the colposcopy images as shown in Fig. 9 (C). The specualr refelction detected and removed on the smart colposcopy images is shown in Table .6. The image inpainting is applied to the detected images to refill the cervical photos using a partial convolutional neural network. The computational time for filling the cervical images is 4 h 28 s with a space consumption of 3.46 Mb.

4.3. Grading of smart colposcopy images

The quality of the cervical images is an important factor during the grading cervical cancer. The grading of CIN1, CIN2 and CIN3, collected from the kaggle, is trained in the pre-trained models like DensetNet121, Vgg19, and efficient model. Similarly, the quality-assessed images are trained using the pretrained model. Based on the analysis, the quality assessed images gives higher accuracy in the grading of cervical cancer, as shown in Table .7. Based on the analysis of the graph the loss value is lower for the enhanced image when compared to the non enhanced images as shown in Table .8.

5. Conclusion

The detection and removal of specular reflection are required to enhance the quality of smart colposcopy images. The proposed binary masking labels the accurate glare region. To automate the process, the U-Net model is used. Finally, partial convolutional inpainting is used to refill the removed portion completely. So this enhancement process has improvised the classification accuracy of the three stages of cervical cancer. It is analyzed using three classification models, DenseNet121, Vgg19, and Efficient Net. Each classification model prediction accuracy is increased in the grading of cervical cancer. So enhancement must be required to improve the grading of cervical cancer on the smart colposcopy images. The proposed binary masking is not limited only to smart colposcopy images. It also predicts glare regions on other medical images captured through digital tools. The limitation faced in this proposed work some time the speculum examination tool on the smart colposcopy images are also identified as the specular reflection. Normally the smart colposcopy device is fixed with the flash light so maximum the images have the same illumination. If the illumination of the image varies the range selection may varies. So it is considered as the limitation for the proposed in the identification of specular reflections. The future scope of the research is to explore how the enhancement has improvised the cancer detection process on smart colposcopy images.

Declaration of competing interest

The authors declare that they have no known competing financial interests or personal relationships that could have appeared to influence the work reported in this paper.

Data availability

The data use is taken from the public database and its link is provided in the manuscript

Acknowledgment

The authors would like to express deep gratitude to the "Centre for Machine Learning and Intelligence" for supporting and sharing the resource for this research work. The Department of Science & Technology supports it under the scheme of DST CURIE AI sanctioned for the "Core Research grant for Artificial Intelligence (AI)" in the year 2021–2023.

References

[1] https://www.who.int/health-topics/cervical-cancer.
[2] S. Zhang, H. Xu, L. Zhang, Y. Qiao, Cervical cancer: epidemiology, risk factors and screening, Chin. J. Cancer Res. 32 (6) (2020 Dec 31) 720–728, https://doi.org/10.21147/j.issn.1000-9604.2020.06.05. PMID: 33446995; PMCID: PMC7797226.
[3] V. Rahatgaonkar, P. Uchale, G. Oka, Comparative study of smart Scope® visual screening test with naked eye visual screening and Pap test, Asian Pac. J. Cancer Prev. APJCP 21 (2020) 3509–3515, https://doi.org/10.31557/apjcp.2020.21.12.3509.
[4] L. Peirson, D. Fitzpatrick-Lewis, D. Ciliska, R. Warren, Screening for cervical cancer: a systematic review and meta-analysis, Syst. Rev. 2 (2013) 35, https://doi.org/10.1186/2046-4053-2-35.
[5] S. Aswathy, M.A. Quereshi, B. Kurian, K. Leelamoni, Cervical cancer screening: current knowledge & practice among women in a rural population of Kerala, India, Indian J. Med. Res. 136 (2) (2012) 205–210.
[6] Y. Jusman, S.C. Ng, N.A. Abu Osman, Intelligent screening systems for cervical cancer, TheScientificWorldJOURNAL (2014), 810368, https://doi.org/10.1155/2014/810368, 2014.
[7] M. Kalbhor, S. Shinde, ColpoClassifier: a hybrid framework for classification of the cervigrams, Diagnostics 13 (6) (2023) 1103, https://doi.org/10.3390/diagnostics13061103. MDPI AG. Retrieved from.
[8] C. Yuan, Y. Yao, B. Cheng, et al., The application of deep learning based diagnostic system to cervical squamous intraepithelial lesions recognition in colposcopy images, Sci. Rep. 10 (2020), 11639, https://doi.org/10.1038/s41598-020-68252-3.
[9] W.H. Huang, R.L. Chen, J.M. Zhang, Improvement and Implementation of Objective Digital Video Quality Measurement, vol. 4, Journal of Beijing University of Posts and Telecommunications, 2005, pp. 87–90, 00.
[10] L. Attard, C.J. Debono, G. Valentino, M.d. Castro, Specular highlights detection using a U-net based deep learning architecture, in: 2020 Fourth International Conference on Multimedia Computing, Networking and Applications (MCNA), 2020, pp. 4–9, https://doi.org/10.1109/MCNA50957.2020.9264278.
[11] A. Das, A. Kar, D. Bhattacharyya, Elimination of specular reflection and identification of ROI: the first step in automated detection of Cervical Cancer using Digital Colposcopy, in: Proceeding of IEEE International Conference on Imaging Systems and Techniques, 2011, pp. 237–241.
[12] Atif Anwer, Samia Ainouz, Mohamad Saad, Syed Saad Ali, Fabrice Meriaudeau, SpecSeg network for specular highlight detection and segmentation in real-world images, Sensors 22 (2022) 6552, https://doi.org/10.3390/s22176552.
[13] V. Pallavi, K. Payal, 'Automated Analysis of Cervix Images to Grade the Severity of Cancer' Annual International Conference of the IEEE Engineering, Medicine and Biology Society, Massachusetts, USA, 2011, pp. 3439–3442.
[14] P. Deepak, K. Philipp, D. Jeff, D. Trevor, A.E. Alecei, 'Context Encoders: Feature Learning by Inpainting' IEEE Conference on Computer Vision and Pattern Recognition (CVPR) 2016, 2016, pp. 2536–2544. Las Vegas, Nevada, USA.
[15] S. Iizuka, E. Simo-Serra, H. Ishikawa, Globally and locally consistent image completion, ACM Trans. Graph. 36 (4) (2017) 1–14.
[16] U. Demir, G.B. Unal, 'Patch-Based Image Inpainting with Generative Adversarial Networks' Computer Vision and Pattern Recognition, 2018 [Online], https://arxiv.org/abs/1803.07422. (Accessed 13 January 2022).
[17] J. Yu, Z. Lin, J. Yang, X. Shen, X. Lu, T. Huang, Free-form image inpainting with gated convolution, in: IEEE/CVF International Conference on Computer Vision (ICCV), 2019, pp. 4470–4479, https://doi.org/10.1109/ICCV.2019.0045, 2019.
[18] Y.L. Chang, Z.Y. Liu, K.Y. Lee, W. Hsu, Free-form video inpainting with 3D gated convolution and temporal PatchGAN, in: 2019 IEEE/CVF International Conference on Computer Vision (ICCV), 2019, pp. 9065–9074.
[19] Triwijoyo, Bambang Krismono, Ahmat Adil, Analysis of medical image resizing using bicubic interpolation algorithm [S.l.], J. Ilmu Komput. 14 (1) (apr. 2021) 20–29, https://doi.org/10.24843/JIK.2021.v14.i01.p03. ISSN 2622-321X. Available at: https://ojs.unud.ac.id/index.php/jik/article/view/69207. (Accessed 6 May 2023). Date accessed:.
[20] O. Ronneberger, P. Fischer, T. Brox, U-net: convolutional networks for biomedical image segmentation, in: N. Navab, J. Hornegger, W. Wells, A. Frangi (Eds.), Medical Image Computing and Computer-Assisted Intervention – MICCAI 2015. MICCAI 2015, Lecture Notes in Computer Science, vol. 9351, Springer, Cham, 2015, https://doi.org/10.1007/978-3-319-24574-4_28.
[21] M.B. Jennyfer Susan, P. Subashini, M. Krishnaveni, Comparison of various deep learning inpainting methods in smart colposcopy images, Int. J. Comput. Intell. Stud. 11 (1) (2022) 53–72, https://doi.org/10.1504/ijcistudies.2022.123347, 2022.
[22] N. Hasan, Y. Bao, A. Shawon, Y. Huang, DenseNet convolutional neural networks application for predicting COVID-19 using CT image, SN computer science 2 (5) (2021) 389, https://doi.org/10.1007/s42979-021-00782-7.
[23] M. Bansal, M. Kumar, M. Sachdeva, A. Mittal, Transfer learning for image classification using VGG19: caltech-101 image data set, in: Journal of Ambient Intelligence and Humanized Computing, vols. 1–12, Advance online publication, 2021, https://doi.org/10.1007/s12652-021-03488-z.
[24] M. Tan, Q.V. Le, EfficientNet: Rethinking Model Scaling for Convolutional Neural Networks, 2019. ArXiv, abs/1905.11946.
[25] Kaggle, Intel & MobileODT Cervical Cancer Screening, & June 8, 2017. November 2022 from, https://www.kaggle.com/competitions/intel-mobileodt-cervical-cancer-screening/overview.
[26] F. van Beers, Arvid Lindström, Emmanuel Okafor, Marco Wiering, Deep Neural Networks with Intersection over Union Loss for Binary Image Segmentation, 2019, https://doi.org/10.5220/0007347504380445.
[27] A critical survey of state-of-the-art image inpainting quality assessment metrics, J. Vis. Commun. Image Represent. 49 (2017) 177–191, https://doi.org/10.1016/j.jvcir.2017.09.006.

Avinashilingam Institute for Home Science and Higher Education for Women
(Deemed to be University Estd. u/s 3 of UGC Act 1956, Category A by MHRD)
Re-accredited with 'A++' Grade by NAAC.CGPA 3.65/4, Category I by UGC
Coimbatore – 641 043, Tamil Nadu, India

PLAGIARISM CHECK REPORT (THESES)

1.	Name of the Research Scholar	Jennyfer Susan M B
2.	Roll No. and Year of Registration	19PHCSF008, 2019
3.	Department	Computer Science
4.	Name of the Research Guide	Dr. P. Subashini
5.	Title of the Thesis / Dissertation	Specular Reflection Removal in Smart Colposcopy Images Using Deep Learning Model for Enhanced Grading of Cervical Cancer
6.	Similarity Content (%) Identified	**6%**
7.	Software Used	Turnitin
8.	Date of Verification	23-04-2024

Note : The report is excluding 14 Consecutive words, Review of Literature and Quoted Materials.

Checked by :

23/4/24
Information Scientist

Research Scholar

23.04.24
Assistant Librarian

23/4/2024
Research Guide

Date: 23-04-2024

Digital Receipt

This receipt acknowledges that Turnitin received your paper. Below you will find the receipt information regarding your submission.

The first page of your submissions is displayed below.

Submission author:	Central Library Avinashilingam
Assignment title:	New 2022
Submission title:	Specular Reflection Removal in Smart Colposcopy Image Usi...
File name:	Thesis_Final_report_version.docx
File size:	12.33M
Page count:	179
Word count:	42,970
Character count:	250,254
Submission date:	23-Apr-2024 03:37PM (UTC+0530)
Submission ID:	2359158492

Chapter 1

Introduction

Cervical cancer is a form of cancer that impacts the cervix, the lower portion of the uterus that connects to the vagina. The abnormal cell growth in the cervix, resulting in the formation of cancer, characterizes this condition. If not treated, it has the potential to metastasize to other region of the body, posing a significant threat to life. According to*World Health Organization* (WHO), in 2020, cervical cancer was identified as the fourth most common cancer among women worldwide [1][2]. The primary cause of this cancer is the Human Papilloma Virus (HPV), which impacts the lower portion of the uterus linked to the vagina. Fortunately, there are ways to prevent cervical cancer by taking the preventive measures like Human papillomavirus immunization and routine screening initiatives [3]. The early detection of cervical cancer allows for effective treatment and cure. However, various factors like anxiety, tension, and economic circumstances, absences of awareness, hesitation, and cultural norms have played a role to its steady rise, especially in developing countries [4].

Stages of Cervical Cancer

It is typically classified into stages based on the severity of the disease. It is categorized into four stages: Stage 0, Stage I, Stage II, and Stage III, each with subcategories to enhance precision[5]. Here's a brief overview of each stage:

Stage 0

- The cervical cancer appears in the lower part of the uterus.
- The cancer is typically small and has not metastasized to nearby tissues or organs.
- It is the primitive stage of cancer and often has the best prognosis when it is detected at this point.

Stage I

- Thecancer has progressed beyond the cervix and uterus but has not reached the pelvic wall, which is the tissue lining the area between your hips or the vagina.
- The cancer may have spread to nearby region but has not yet reached distant organs.

1

Specular Reflection Removal in Smart Colposcopy Image Using Deep Learning Model for Enhanced Grading of Cervical Cancer

by Central Library Avinashilingam

Specular Reflection Removal in Smart Colposcopy Image Using Deep Learning Model for Enhanced Grading of Cervical Cancer

ORIGINALITY REPORT

6%	2%	5%	2%
SIMILARITY INDEX	INTERNET SOURCES	PUBLICATIONS	STUDENT PAPERS

PRIMARY SOURCES

1	M.B. Jennyfer Susan, P. Subashini. "Improvising grading of cervical cancer using quality assessment method in smart colposcopy images", Measurement: Sensors, 2023 Publication	<1%
2	"Inventive Communication and Computational Technologies", Springer Science and Business Media LLC, 2023 Publication	<1%
3	Submitted to Liverpool John Moores University Student Paper	<1%
4	www.researchgate.net Internet Source	<1%
5	"Medical Image Computing and Computer Assisted Intervention – MICCAI 2018", Springer Nature America, Inc, 2018 Publication	<1%